THE SURFACE TENSION OF SOLID NICKEL

by

EINO SAAREMAA

A THESIS SUBMITTED IN PARTIAL FULFILLMENT OF THE
REQUIREMENTS FOR THE DEGREE OF
MASTER OF APPLIED SCIENCE
in the
Department of Mining and Metallurgy
at the
University of British Columbia.

We accept this thesis as conforming to the standard required from candidates for the degree of 'Master of Applied Science' in Metallurgical Engineering

Members of the Department of Mining and Metallurgy
THE UNIVERSITY OF BRITISH COLUMBIA

JANUARY, 1957.

ABSTRACT

The surface tension of solid commercially pure nickel was determined by the force measurement technique using fine wires as proposed by Udin, Shaler, and Wulff. Grain boundary measurements were also made on the same metal.

After finding experimentally that tests in a vacuum of approximately 5×10^{-5} mm Hg were unsuccessful because of the high power vapour pressure of nickel at high temperatures, similar tests were made in helium and argon atmospheres, the pressure being kept constant at 760 mm Hg during the experiments.

The average surface tension of nickel in argon was found to be 2220 ± 300 dynes per centimeter for a temperature range from 1370°C to 1390°C.

The relative grain boundary energy of solid nickel was determined by measuring the dihedral grain boundary groove angles of thermally etched nickel. The interferometric method developed by Hilliard and Harrold was used for this purpose. An average value of 161 degrees was found for the dihedral angle. The grain boundary energy was calculated to be 740 ± 300 dynes per centimeter.

Examination of thermally etched nickel surfaces was inconclusive with respect to physical evidence for dislocation.

In presenting this thesis in partial fulfilment of the requirements for an advanced degree at the University of British Columbia, I agree that the Library shall make it freely available for reference and study. I further agree that permission for extensive copying of this thesis for scholarly purposes may be granted by the Head of my Department or by his representative. It is understood that copying or publication of this thesis for financial gain shall not be allowed without my written permission.

Department of Mining and Metallurgy

The University of British Columbia,
Vancouver 8, Canada.

Date January 24th, 1957

ACKNOWLEDGMENT

The author is grateful to the National Research Council and Defence Research Board of Canada for financial aid in the form of a Research Assistantship granted during the past year.

The work was carried out with the help of funds provided by the Defence Research Board of Canada.

The experimental work was done in the laboratories of the Department of Mining and Metallurgy, and the author wishes to thank Professor F.A. Forward, Head of the Department, for the facilities and the assistance made available to him. Special thanks are extended to Dr. Vernon Griffiths, the director of this research, and to R.G. Butters for technical advice and encouragement.

Thanks are extended to Professor A.M. Crooker, of the Physics Department, for providing the facilities to prepare the partially reflective optical flats.

TABLE OF CONTENTS

TABLE OF CONTENTS (cont'd.)

LIST OF ILLUSTRATIONS

LIST OF ILLUSTRATIONS (cont'd.)

LIST OF TABLES

THE SURFACE TENSION OF SOLID NICKEL

I. INTRODUCTION

The present work on solid nickel was motivated by the growing need for numerical values of the surface tension of solids, as a result of increasing interest in the role of interphase boundary phenomena in metals.

The existence of surface tension forces in solids has been known for almost a century. Only very little progress was made in the study of this phenomenon up to 1948 when C.S. Smith[1] extended to multiphase alloys the idea of D. Harker and E.R. Parker[2] that crystal growth in heated metals is due to grain boundary forces. Smith also showed the nature of the dependence of crystallite shape on interfacial tensions between solidified crystals and still liquid alloy. Since some of the mechanical properties of engineering alloys are structure sensitive, many metallurgists were alerted by this paper.

Hollomon and his co-workers realized that the phase nucleation theory of Volmer,[3] extended by Becker[4] to solid-state transformation, required some data on solid surface tension to activate it to practical use.

In the study of sintering of metal powders it was found that a more basic understanding of the operating mechanisms was needed for further development. Shaler[5] showed that an exact value of surface tension of solid metals is

necessary for solution of the kinetics of sintering, because this force plays a principal role in densification and strengthening of powder compacts.

Welding metallurgists realized that surface forces determine the soundness of welded or brazed joints. G.L.C. Bailey and H.C. Watkins were led to a study of the surface forces in metals by their interest in the joining of metals.

Besides the metallurgists, chemical engineers interested in catalysis, mechanical engineers working on lubrication problems had shown appreciation of the importance of the surface forces in metals, but had been unable to determine experimentally the solid:liquid and solid:gas interfacial tensions.

The surface forces (definitions and terms used are given in Appendix A) are a direct result of chemical free energy. The interfacial atoms are at energy states between those of interior atoms and vaporized atoms. The difference between the energy of surface atoms and internal atoms is in terms of the energy required to form a unit area of the surface, and is called surface energy. This excess energy in the surface provides the driving force for any process which may induce a decrease in surface area. Such a process is capable of doing work at the expense of the energy of decreasing surface.

Gibbs[6] has proved that this excess energy at the interface between two phases is a partial function of the

interfacial area, thus $\frac{\partial F}{\partial S} = \gamma$

where $\frac{\partial F}{\partial S}$ is the rate of change of free energy of the system with changing surface area at constant temperature, pressure, and composition.

γ is the interfacial force per unit length or free energy per unit area, being expressed either in dynes/cm or in ergs/cm.^{2}

Therefore, two approaches are possible to measure the surface energy of the solids. The surface tension may be determined either by thermodynamic measurement of the surface energy or by a mechanical measurement of the surface force by the application of a balancing counterforce.

At present the values of the surface forces of Cu, Au and Ag, all being metals of relatively low melting points, have been determined by the use of the second method.

The present work to determine the surface tension of solid nickel is an attempt to use the force measurement technique first developed by Udin and his collaborators, on a metal of higher melting point.

II. PREVIOUS WORK

Experimental Techniques

Energy measurements.

Thermodynamical measurements to determine surface energy have been carried out by the application of heat-of-

solution method. Fricke and Meyer[7] measured the heat of solution of massive gold in iodine trichloride, and found it to be lower than that of fine gold particles. Surface area was evaluated on the basis of cubic particles, the diameter of the particles being determined from the amount of broadening of the x-ray diffraction lines of the gold powder. This area and the excess heat of solution yielded a surface energy equal to 670 ergs per square centimeter.

Hüttig and his collaborators[8] determined the interfacial tension copper:copper sulphate to be 40,000 ergs per square centimeter by measuring the electromotive force between electrodes of copper powder and massive copper respectively, in a copper sulphate solution. Since copper tends to dissolve from the powder electrode and precipitate on the massive metal, an equilibrium emf. due to the excess solution tension of particles of radius r, and with an interfacial tension γ against the electrolyte, can be measured.

$$V = \frac{2M\gamma}{Fr\rho}$$

where $\frac{M}{\rho}$ is the ratio of atomic weight to density of the particle

F is Faraday's constant.

Certain errors are introduced in estimating the surface area or particle size, and in using the electrochemical method, due to the side reactions and non-equilibrium conditions.

Force measurements

The techniques for determining the force of surface

tension have been more favored than those involving measurement of energy, because of fewer experimental difficulties and uncertainties. These methods involve the balancing of surface tension with a counterforce. Thin wires or foils are loaded with weights of varying magnitude and heated to a temperature below the melting point. The strains (positive if due to the counterforce, and negative if due to the surface tension) are observed. The load which exactly balances the upward pull of the surface tension is estimated from the plot of strain against stress. The interpolated load allows the determination of the value of the surface tension in a simple calculation.

This technique has been known for many years, and surface tension values have been reported by Chapman and Porter,[9] Schottky[10] and Berggren[11] in the earlier part of the century. The filament technique was later used successfully to determine the surface tension of viscous liquids. Tammann and co-workers,[12, 13] Sawai and collaborators,[14,16] and Mack[17] reported good agreement between this technique and more conventional methods of measuring the surface tension of glasses and tars.

All these experimental results supported the belief in reliability of the technique and soon it was employed with success on solid metals. Sawai and Nishida,[18,19] and Tammann and Boehme[20] made quantitative measurements on gold foils and attempted to calculate from their results the interfacial tension of the non-equilibrium system gold:air.

In experiments for determining the surface tension, loaded wires rather than loaded foils may be used, although the

sensitivty of the test is somewhat diminished due to the unfavorable surface area to cross-sectional area ratio of thin wires. For example, Sawai's gold foils being 7.7×10^{-5} centimeters thick, were subjected to a shrinkage stress of 19 kg. per square centimeter at a surface tension of 1500 dynes per centimeter, whereas in 0.008-centimeter radius wire the stress is only 0.37 kg. per square centimeter. Hence, the use of wires in the experiments requires an operation very near the melting point for a reasonable duration. The insensitivity in using wires is counterbalanced by the following considerations. The cylindrical wire, in equilibrium, is in a state of hydrostatic compression, the strain rate in all directions being zero, which is not true in the case of foils. Secondly, the grain boundary energy, undoubtedly one of the components of the force acting on the specimens, can be dealt with in case of wires, if the majority of grain boundaries are perpendicular to the wire axis. Finally, strain anisotropy is negligible in the case of wires as compared to foils.

Consider a wire of length l and radius r containing n + 1 grains with a cross-section equal to that of the wire with boundaries perpendicular to the axis of the wire (Fig. 1).

If the shrinkage force of the surface tension is just counterbalanced by a suspended weight W, then the axial stress

$$\sigma_x = \frac{W - 2\pi r\gamma}{\pi r^2} \qquad (1)$$

where γ is the surface tension of the wire, the x-axis being along the wire with tension positive.

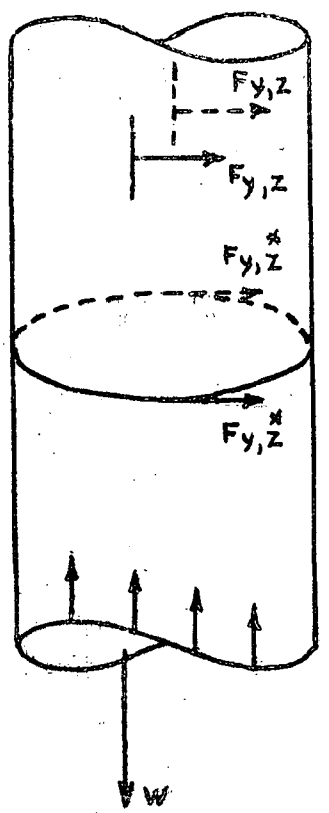

Fig. 1. The Stress Analysis of Loaded Wire

The stresses perpendicular to the wire are due to the circumferential force of the surface tension and the line forces due to each grain boundary. These forces are equal and can be expressed by

$$\sigma_y = \sigma_z = -\left(\frac{\gamma}{r} + \frac{n}{\ell}\gamma^*\right) \qquad (2)$$

where γ^* is the grain boundary tension.

For the case of zero strain in the x-direction, the strain will also be zero in the y- and z-directions, since the wire is under hydrostatic stress. Hence $\sigma_x = \sigma_y = \sigma_z$ and thus

$$w = \pi r \gamma - \frac{n}{\ell} \pi r^2 \gamma^* \qquad (3)$$

From this equation the surface tension can be determined in a single experiment if the grain boundary tension is known, or if the ratio of grain boundary tension to surface tension is available.

Udin, Shaler, and Wulff[21] first applied this technique to evaluate the surface tension of copper in vacuum. Their value for the surface tension of solid copper was 1670 dynes per centimeter at 1050°C, as corrected by Udin[22] according to the Equation 3. The results are summarized graphically in Fig. 2, and a typical stress-strain diagram is shown in Fig. 3.

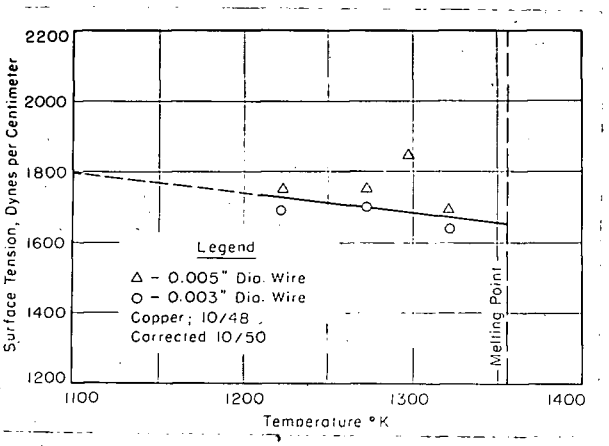

Fig. 2 Surface Tension of Solid Copper as a Function of Temperature (after H. Udin).

Funk, Udin, and Wulff[23] experimented on silver in a helium atmosphere, after they found that the vapor pressure of silver was too high to attain the metal:vapour equilibrium in their experiments in vacuum. The surface tension of silver in helium was found to be 1140±90 dynes per centimeter for the temperature range from 875° C to 932° C, which is a true surface tension, because helium is insoluble in silver and will not be physically adsorbed at high temperatures, and cannot chemisorb to a metal surface.

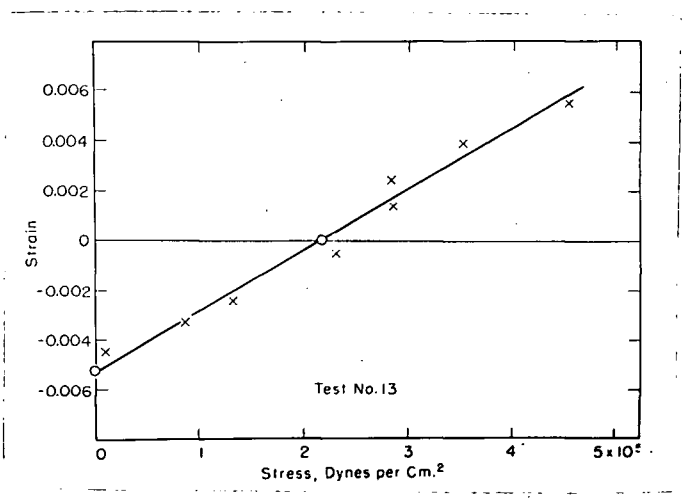

Fig. 3. A Typical Experimental Stress-Strain Diagram (after H. Udin).

Alexander, Kuczynski and Dawson[24] who worked with gold wires suspended in tubular nickel heaters in vacuum, had similar difficulties. Since a complex gold:gold vapor:nickel vapor system with no possibility of gold:gold vapor equilibrium was used, no reproducible values for the interfacial tension of the system were obtained.

Buttner, Udin and Wulff[25] experimented on gold wires in helium atmosphere to determine the surface tension of solid gold. They determined a value of 1400±65 dynes per centimeter for the temperature range from 1017°C°to 1042°C.

Buttner, Funk and Udin[26] studied the effect of oxygen on surface tension. They found the interfacial tension of the system gold:gold vapor:air at 1040°C to be 1210 dynes per centimeter as compared to 1370 dynes per centimeter for the system gold:gold vapor at the same temperature; and the interfacial tension of the system silver:silver vapor:air at 930°C only 450 dynes per centimeter as compared to 1140 dynes per centimeter for the surface tension of silver. Since the experimentally determined values are accurate only to about ±5%, no further experiments were carried out in the case of gold. The effect of oxygen on surface tension of silver was studied more fully. Tests were run in various mixtures of purified helium plus dried electrolytic oxygen. The results showed a linear relationship between surface tension and the logarithm of oxygen partial pressure. It was concluded that silver will adsorb approximately 1.7×10^{15} atoms of oxygen per square centimeter of surface, the amount not being dependent on pressure in the range investigated, and form a surface-stabilized film of oxide.

The experimental technique is a delicate one. The marking of reference points on the wire presents a difficult problem. Painting or plating the wires outside a given gage length is not satisfactory because anything adhering to the

surface lowers the surface energy. Knotting the wires at two points was used by Udin and co-workers in the case of copper. The gage points are taken as intersection of the inner loops of the knot with the straight portion of the wire (Fig.4).

Later Udin and his group inscribed the marks by rotating the wire mounted in a jeweler's lathe against a pair of razor blades spaced the required gage length apart.

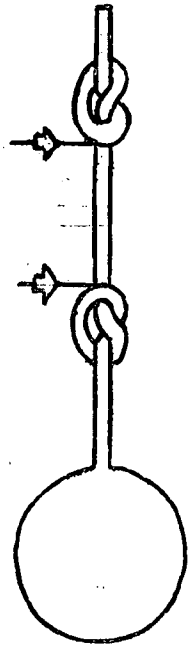

Fig. 4 A Drawing Showing the Marking of Reference Points on the Wire.

The weights, ranging from zero to about two to three times the estimated weight required for balance, are fused to the ends of the gage-marked wires. Eight to sixteen wires used

in each test are suspended from the lid of the metal cell. The weights, lid, and the box are made of the same metal used for the specimen. Thus at temperature the wires hang in an equilibrium with metal vapor atmosphere.

The wires are straightened and annealed at or above the experimental temperature for at least one hour in the vacuum or test atmosphere. After cooling, the specimens are removed to measure the gage length and count the grains. The assembly is returned to the furnace and held at the test temperature for a time sufficient for measurable creep to take place, the time being dependent on the temperature and accuracy required. The furnace is cooled to room temperature, the specimens are removed and re-measured. It has been found that no further grain growth takes place during the test because the thermally etched grooves produced during the anneal anchor the grain boundaries.

The change in length is transformed to engineering strain and plotted against the stress due to the suspended weights, which are corrected by taking into account the weight of the wire below the point midway between the upper and lower gage marks. The intercept of this plot with the strain axis gives the value of the stress at zero strain or the value of w from Equation 3,

$$w = \pi r \gamma - \left(\frac{n}{2}\right)\pi r^2 \gamma^*$$

Grain boundary energy measurements.

In order to calculate the surface tension for the given metal, either the value of the grain boundary energy

must be known, or the ratio between γ^* and γ assumed. Up to 1948 no satisfactory methods to determine the interfacial energies, such as grain boundary energy, were available. A new attack to the problem was proposed by C.S. Smith[1] who showed that the geometrical shapes of grains result from an approach to an equilibrium between phase and grain interfaces whose surface tensions geometrically balance each other at the points and along the lines of contact when annealed at sufficiently high temperatures for a sufficient length of time. This relationship between grain boundary tensions and grain boundary geometry had been suggested earlier by Desch.[27] Measurement of angles established between the interfaces when in equilibrium, provides a method to determine the relative values of surface forces involved according to the relationship

$$\frac{E_1}{\sin\psi_1} = \frac{E_2}{\sin\psi_2} = \frac{E_3}{\sin\psi_3} \qquad (4)$$

Where E's are the respective specific interfacial energies, and ψ's are the dihedral angles between the interfaces measured in the plane perpendicular to the junction. However, this relationship will be complicated by the orientation dependence of grain boundary energies. The evidence available concerning the orientation dependence of solid interface energies is sparse but it seems that both experimentally and theoretically its effect may be expected to be small, except for a limited number of cases when grain boundaries have cusp orientations.

Physical measurement of microscopic dihedral angles

is difficult because, by definition, they must be measured in a plane perpendicular to the line of junction of the interfaces, which actual direction is unknown. Harker and Parker[2] proposed a statistical method which, if employed, would give the value of dihedral angle within the limits of $\pm 5^{\circ}$ when a large number of dihedral angles were measured at random. This method has been used in some cases with certain modifications by different researchers.

A more subtle method is the calibration of solid:solid interfacial tension in absolute units when the energies of such solid:liquid or solid:gas surfaces are known or can be determined by the methods described above. Calibration with solid:gas tension is preferred to the calibration with a solid:liquid tension because an inert gas or vacuum can be used to avoid contamination of the interface under study. During the equilibrating heat treatment, shallow grooves on the free surface of the specimen at the grain boundaries are formed, the process being called 'thermal etching'. If the dihedral or groove angles Ψ are measured and the surface tension of the solid in the gas is known, the grain boundary energy can be calculated from the formula (Fig. 5)

$$\gamma^{*} = 2\gamma \cos \frac{\Psi}{2} \qquad (5)$$

Or, subsequently, if the surface tension and grain boundary tension are determined simultaneously, the two unknowns γ and γ^{*} may be calculated from

$$\begin{cases} w = \pi r \gamma - \left(\frac{n}{2}\right)\pi r^2 \gamma^* \\ \gamma^* = 2\gamma \cos\frac{\psi}{2} \end{cases} \qquad (6)$$

where all other values can be measured.

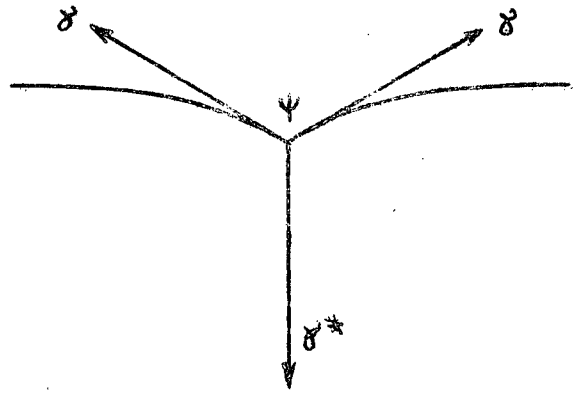

Fig. 5 Dihedral Groove Angle of a Thermally Etched Specimen.

Because of the small size of the grooves (approx. 1 micron deep) and the obtuseness of the groove angle (usually 160 degrees or greater), a small experimental error in measuring the angle produces a large relative error in the calculated grain boundary energy, the experimental technique is difficult.

Bailey and Watkins[28] measured the groove angles of thermally etched copper in microsections taken normal to the surface. Buttner, Udin and Wulff[29] determined the absolute grain boundary energy of gold at 1300°K to be 365±50 dynes per centimeter by measuring dihedral angles. Greenough and King[30] used both microsections and taper-sections to measure dihedral groove angles in silver, and checked their results successfully by a method of optical goniometry. The latter method, however,

is not sufficiently accurate because of the very small size of the groove and continuous curvature of the groove surfaces and of the magnitude of the wave length of light. Fullman[31] determined the groove angle for copper coherent twin boundaries thermally etched in lead vapor and demonstrated that there is an optimum taper-sectioning angle for most accurate measurement of a particular groove.

Hess[32] and others[33] used the method of multiple-beam interferometry developed by Tolansky[34] to measure the groove angles of pure copper but found that large errors in the calculated grain boundary energies result, if the reference plate and the surface deviate from parallelism more than approximately 2 degrees. On the other hand, Hilliard[35] has demonstrated that the interferometric method is sufficiently accurate, if the reference plate and the experimental surface are parallel, by measuring grain groove angles in the Cu-Au system.

This method consists in matching an aluminized or silvered, optically flat, glass surface of reflectivity approximately 0.50 against the metal surface, and the use of monochromatic light in the formation of Fizeau fringes which represent the contour lines in the surface topography. Knowing the necessary constants, the elevation profile of the surface slope in the grain boundary may be constructed and the dihedral angle measured. The equation governing fringes of minimum reflection from the interferometric gap s, is

$$2\pi \frac{2s}{\lambda} + \varepsilon = (2n+1)\pi \qquad (7)$$

according to Harrold[36] who used glass slips coated with multiple dielectric films. When the objective is focused in the air gap between the reflective surface of the optical flat, the metal specimen reveals contour lines at intervals of $\frac{\lambda}{2}$ as S varies with irregularity of the metal surface and assumes successive integral values. ε, the sum of all relevant phase changes at reflection, is fixed in this case.

No critical evaluation for the interferometric method developed by Hilliard and Harrold is available at the present. However, present work has demonstrated convincingly the applicability and the relative simplicity of the method with respect to other conventional techniques. This method makes it possible to pick the grain boundary grooves suitable for the measurement of dihedral angles by observing the symmetry of the Fizeau fringes. No time-consuming work is required as in the case of microsections, or determining the dihedral angle by the use of statistical methods. Furthermore, the accuracy of the method is believed to be higher than that of the other methods because of the fewer experimental difficulties and uncertainties involved.

Theoretical Considerations.

Viscosity

Knowing the surface tension of solid metals, it is possible to calculate their viscosity, if certain assumptions are made. It is assumed that the material contracts or extends uniformly along the length of the specimen, and also that it flows in a viscous fashion, i.e. that the strain rates are

proportional to the stress applied. If viscous flow is assumed, no change in lattice energy should be present, and all the strain energy should appear as heat. The kinetic energy of the moving weight being neglected, the time rate of heat generation equals the rate of change of potential energy by changing both the position of the weight and the area of the metal surface. Therefore, under isothermal conditions,

$$\frac{dQ}{dt} = w\frac{dl}{dt} - \gamma\frac{ds}{dt} \tag{8}$$

where Q is the heat of viscous flow.

According to Frenkel[37] the energy dissipated in flow for a viscous rod under longitudinal strain is

$$\frac{dQ}{dt} = \frac{6\eta V}{l^2}\left(\frac{dl}{dt}\right)^2 \tag{9}$$

where η is the coefficient of viscosity

By making necessary substitutions, a simplified relationship

$$\epsilon = \frac{t}{6\eta}\left(\sigma - \frac{\gamma}{r}\right) \tag{10}$$

is derived, if the strains measured are small, σ being stress.

Udin has calculated the coefficient of viscosity from his experimental data on surface tension of copper using equation 10, and plotted the logarithm of the viscosity against the reciprocal of absolute temperature. The equation of the resulting line is

$$\eta = 130\, e^{\frac{59000}{RT}} \tag{11}$$

The activation energy of 59,000 calories per mole is within the

range of values reported for self-diffusion of copper by Steigman.[39] However, the constant is 10^7 times larger than that predicted by Kauzmann[38] according to the equation

$$\eta = \frac{h}{\lambda^3} \frac{RT}{Q} e^{\frac{Q}{RT}} \qquad (12)$$

Udin concluded that an atomic vacancy is the unit of flow, but only a very small fraction of vacancies can participate in the flow.

Herring theory of diffusional viscosity.

Since the correctness of the reported values for surface tension of various metals and the future experimental work is based on the assumption that the specimens deform in a viscous fashion, it is necessary that a mechanism be established that would explain both the viscous flow and the uniform deformation. Such a mechanism has been proposed by Herring[40] who explains the deformation taking place under experimental conditions by means of a flow of vacancies between grain boundaries and surfaces. This theory, which is a direct but independent extension of the theory put forward by Nabarro[41] in an attempt to explain the microcreep observed by Chalmers in single tin crystals, suggests that any crystal can change its shape by self-diffusion in such a way as to yield to an applied shearing stress. This can cause the macroscopic behaviour of a polycrystalline solid to be like that of a viscous liquid. It is assumed that this phenomenon is the predominant cause of creep at very high temperatures and very low stresses, though not under normal conditions. It is pointed out that a polycrystalline solid under a shearing stress, can, because of

self-diffusion within the grains, yield as a result of diffusional flow of matter within each crystal away from grain boundaries where there is a normal pressure, and towards those where there is a normal tension. The yielding is macroscopically describable by an effective viscosity proportional to the square of the linear dimensions of the grains. This theory of so-called 'diffusional viscosity' provides a possible explanation for the behaviour which has been observed for foils and wires being suspended with very small loads and held at an elevated temperature.

The rate of yielding of the specimen to the applied forces understandably depends on the detailed distribution of the sizes and shapes of its crystal grains, and on whether or not the grain boundaries are able to withstand shearing stress for times as long as are necessary for measurable diffusional flow to take place. It has been found that shearing stresses across metallic grain boundaries are rapidly relaxed at high temperatures, which seems to be a general property of grain boundaries. The rate of creep, until this relaxation has become complete, will usually be considerably faster than that due to diffusional viscosity.

Compared to the stresses in ordinary creep experiments, the low stresses used in experiments to determine the surface tension of metals indicate that the mechanism proposed by Nabarro and Herring to explain the deformation of the specimen is most probable, although it is, of course, quite conceivable that the mechanism of ordinary creep and microcreep are the

same, the threshold being lower and the rates faster at the higher temperatures.

Herring's viscosity equation for a wire with 'bamboo-like' structure is

$$\eta = \frac{2\ kTRL}{3\ BD\Omega_o} \qquad (13)$$

where T is the absolute temperature

R is the radius of the grain

L is the length of the grain

D is the self-diffusion coefficient

B is a function of grain shape $\frac{L}{R}$

Ω_o is atomic volume

The theory was verified by the work of Udin and others[42] who determined that the viscosity of 5 mil gold wires is much higher than that of 1 mil wires. Good agreement with theory was also found by Greenough[43] who observed strain rates in silver single crystals. Opposed to these observations were the results of Udin and his collaborators[21] on solid copper in which case the viscosity was found to decrease as grain size increased.

A series of experiments were carried out by Pranatis and Pound[44] with copper foils of varying grain size to confirm the Herring theory of diffusional viscosity. A good agreement between calculated and observed values of the coefficient of viscosity, activation energy, and self-diffusion coefficient was found. This additional evidence in favor of Herring's theory of viscous flow indicates that the values of surface tension

obtained by force measurement techniques may be regarded with confidence. The relationships determined between viscosity and grain size, and viscosity and temperature, as well as the values of observed viscosities, strongly support the proposal that deformation under the experimental conditions develops almost entirely by means of vacancy diffusion. Slip, kinking, offsetting, and grain boundary sliding are assumed to make only limited contributions.

Theories of surface tension of solids

Not only are the available data concerning the numerical values of the surface tension of solids incomplete, but in addition, no satisfactory theory of the surface tension of nonionic solids is available at present. Stratton's[45] electron theory of surface tension of solid metals is one of the best of the existing ones, but its predictions are considerably lower than the experimentally known surface tensions of liquid metals, and hence has to be considered at least in its quantitative predictions inadequate.

Lately a new theory of surface tension of solids based on the elementary next-neighbor approach has been presented by Skapski.[46] This theory allows one to calculate the surface tension of non-ionic solids from the arrangement of next neighbors, from the heat of fusion, and from the surface tension of the liquid substance at the melting-point. Comparison of the theoretical values with experimental data obtained from foil- or wire-stretching experiments has given good agreement.

III. EXPERIMENTAL

Materials

Commercially pure nickel of Type "A" grade was supplied by Johnson and Matthey Company Ltd., London, England. This was in the form of 1/2" round bar for grain boundary energy measurements and 1/8" wire for surface tension measurements. The analysis for this material is given in Appendix B. In the latter stages of the experimental work, nickel wire of 0.010 inch size manufactured by Hoskins Alloys Canada Ltd., Toronto, became available.

Equipment

The vacuum furnace (Fig.6) used in the experimental work was of mild steel, with a diameter of 8 inches and a height of 20 inches, inside dimensions. It was evacuated by a 275 liter/sec oil diffusion pump backed by a 140 liter/min mechanical pump.

Pressure was measured by a thermocouple vacuum gauge, and by an ionization gauge. The vacuum measuring unit allowed an effective range from 1 mm to 10^{-7} mm Hg, and pressures of 2×10^{-5} mm Hg were readily obtained.

One platinum thermocouple, used for controlling the temperature, and the power leads were inserted through the furnace arm which was specially designed for that purpose. The other thermocouple was introduced into the furnace through the bottom plate of the furnace. The controlling thermocouple was connected to a Honeywell recorder-controller and the emf. of the

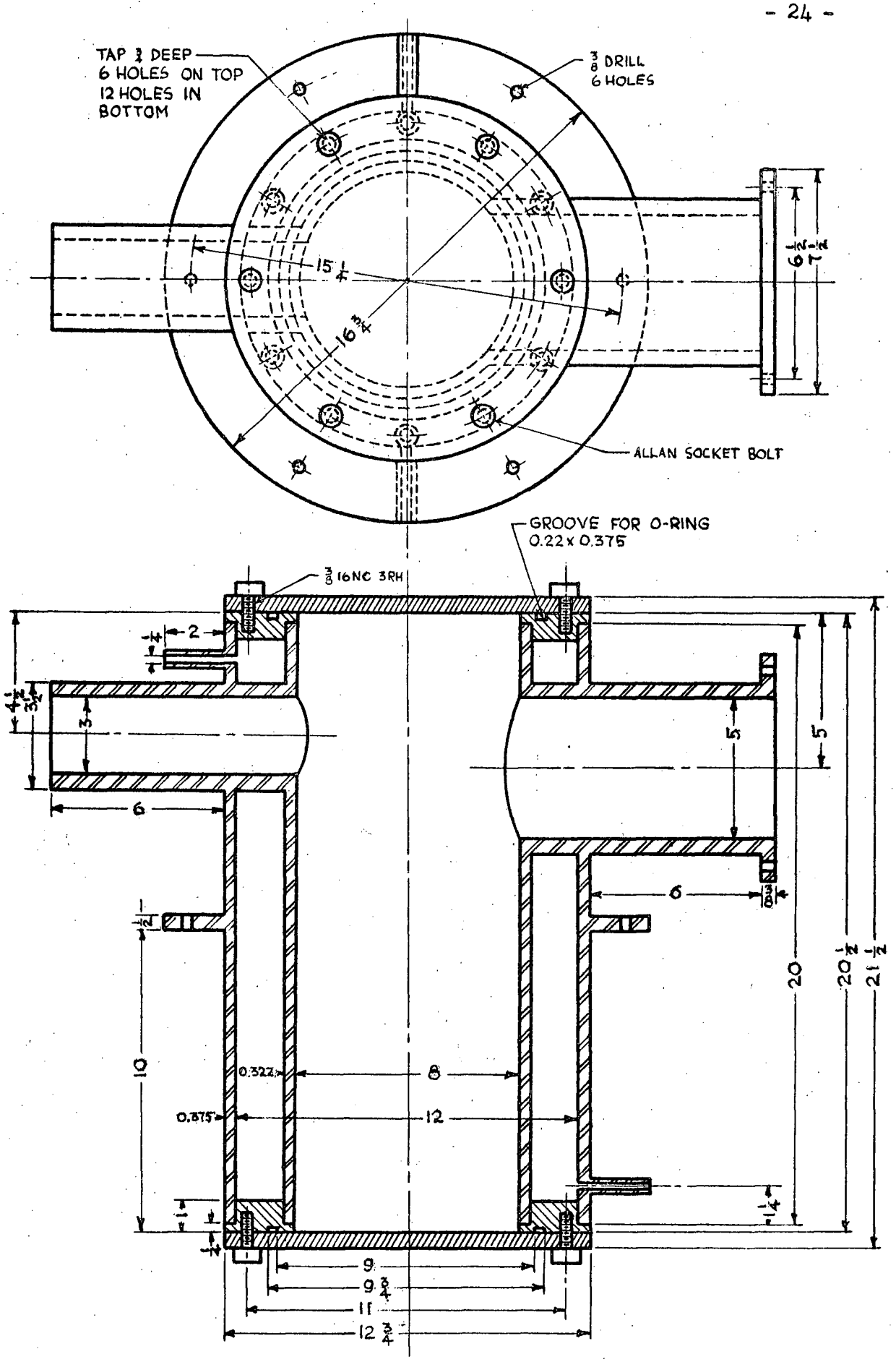

Fig. 6 Vacuum Furnace

other thermocouple was measured with a Tinsley potentiometer.

A heating coil of molybdenum 0.025 inch wire, wound on a grooved alundum tube 12 inches long and of $1\frac{1}{4}$ inch diameter, supplied the furnace with power.

Heat losses by radiation from the heated zone were decreased by the use of three concentric radiation shields made of molybdenum sheet.

Figure 7 shows the interior arrangement of the furnace. A complete drawing of the electrical power supply, thermocouple, and vacuum gauge circuits is given in Appendix C.

Procedures.

Nickel wires of 0.010 inch diameter were prepared by drawing the 1/8 inch wire with jeweler's drawing plates. It was found necessary to anneal the cold worked wires quite often. The best lubricant for the work was thin lubricating oil for scientific instruments. After every individual step of reduction, the wires were cleaned thoroughly with carbon tetrachloride, and annealed in hydrogen at about 1200°C for approximately 30 minutes. Steel boats filled with fine alundum powder were used in this operation. The process was repeated until the minimum size of the wire was established.

The Udin technique of force measurement was used. Nickel wires of 0.010 inch diameter were cold worked about 3% by stretching and then annealed to grow sufficiently large grains. The most effective range of cold working was obtained

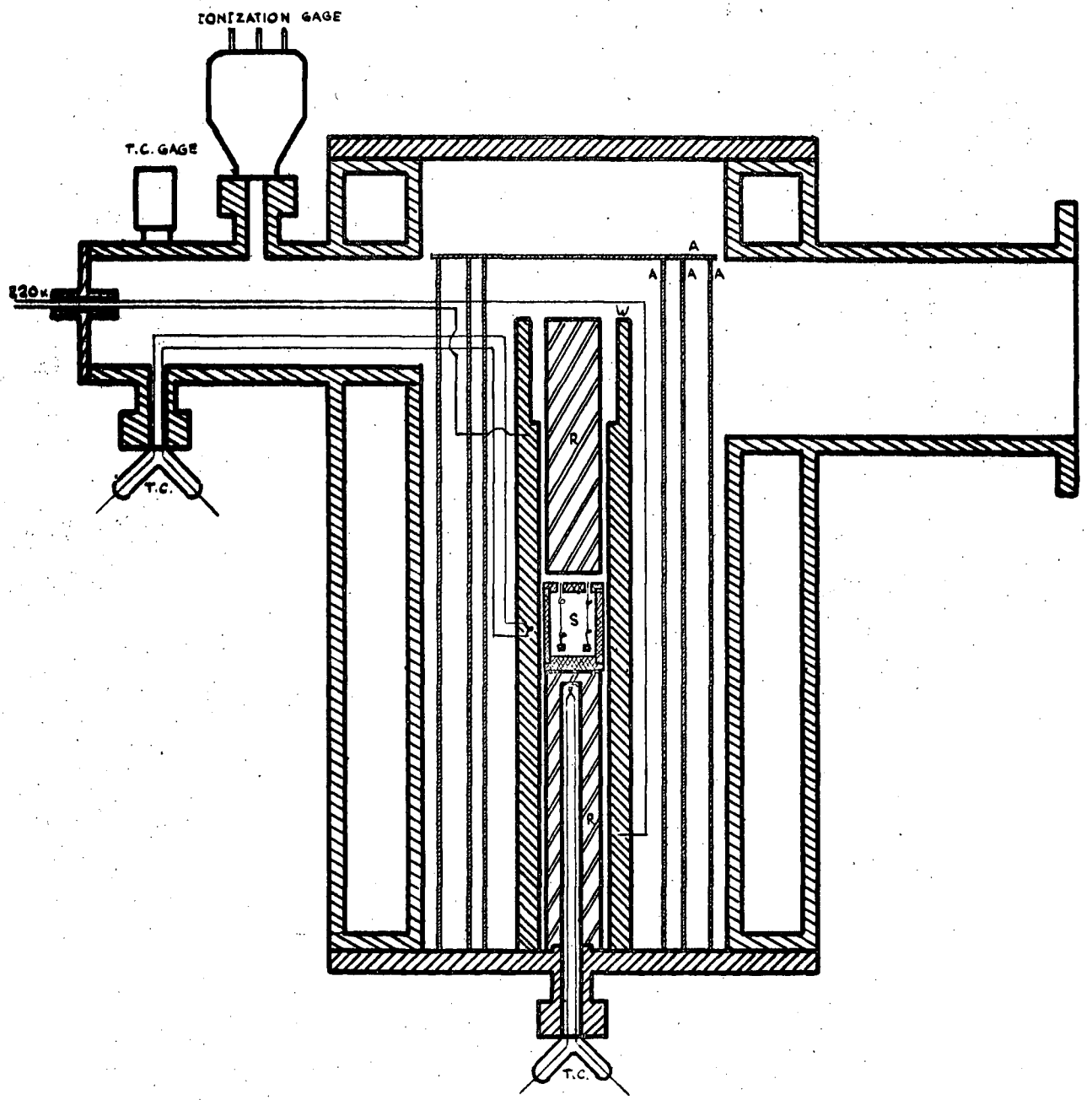

Fig. 7 Interior Arrangement of the Vacuum Furnace

A - Radiation shells
R - Refractory
S - Specimen
W - Winding tube
T.C. - Thermocouple

experimentally by stretching wires at different rates of strain and determining microscopically the effects.

The wires, cut to suitable lengths, were knotted at two points leaving the approximately predetermined gage length between them. Great care was taken in making the knots in order to minimize cold working of the wire between the knots.

A load of known weight was attached to each wire. The weight, ranging from zero to about two to three times the estimated weight required for balance, had a hole drilled in its center. The wire was pushed through the hole and then secured by making another knot below the load. The other end of the loaded wire was pushed through the hole in the top of the nickel box, and wedged there by a small nickel plug. After seven or eight wires were mounted to the top of the box, the top was attached tightly to the box, after making sure that the wires and the weights touched neither each other nor the walls of the box. The box together with the top plus wires and the removable nickel bottom was introduced into the furnace using a small electromagnet.

The wires were annealed and straightened at or above the experimental temperature in a vacuum of 5×10^{-5} mm Hg for approximately one hour. The furnace was cooled to room temperature, a process requiring about twelve hours. After the nickel box was removed from the furnace with the electromagnet, the gage lengths of the wires, still attached to the top of the box, were measured with the travelling horizontal microscope, and the grains were counted. The box was reassembled, returned

to the furnace, and brought to the experimental temperature for a time sufficiently long for a measurable creep to take place, this time being longer the lower the temperature. The furnace was cooled again to room temperature, specimens were removed and re-measured. The change in length was converted to engineering strain, and plotted against stress arising from the suspended weights.

To measure the grain boundary energy of solid nickel, the following work had to be carried out.

Glass proof plates of 1 mm thickness were tested against a standard optical flat, and the satisfactory ones were picked out. These glasses were cleaned thoroughly in nitric acid and washed with distilled water and soap. They were dried carefully and mounted five at a time on a specially prepared support. Aluminum was evaporated in a suitable apparatus. The determination of the thickness of the film for fifty percent transmission and the weight of the coating material are shown in Appendix D. A complete description of the apparatus and the procedure used in silvering the mirrors is given by Strong.[47] For this work the apparatus from the Physics Department of the University of British Columbia was kindly made available. Aluminum was used as a coating material since silver was considered to be unsatisfactory because of its tendency to form sulphides; the multiple dielectric films proposed by Harrold[36] were not used because of the experimental difficulties in preparing them. Optical flats were produced with the following reflectivities: 20%, 30%, 40%, 50%, and 70%.

Pieces approximately 1/2 inch long were cut from a commercially pure nickel bar of 1/2 inch diameter, cold worked three percent by compression and polished according to the best conventional methods. These specimens were annealed in vacuum for a few days in the temperature range from 1200°C to 1300°C. The prior cold work of the specimens allowed the grains to grow to a sufficiently large size, and to reach thermodynamical equilibrium at the experimental temperature during the time allowed. After the furnace was cooled to room temperature, the specimens were removed for microscopic observation of the thermally etched grain boundaries.

The contour fringes of the grain boundary grooves were visible in monochromatic light, when the thermally etched metal surface was observed through the partially reflecting optical flat with its coated surface against the specimen, provided that the reference plate and the surface of the specimen were parallel. The mercury green line of wave length 5461 Angstroms used was obtained from an interference filter made by Barr and Stroud. The objective, focused in the air gap, revealed the contour lines at intervals of $\lambda/2$ as the interferometric gap varied with the irregularity of the metal surface. The field of view was photographed to study the surface profiles obtained from the fringes of equal chromatic order. By the application of experimental data in the calculations, the profile of the grain boundary groove was plotted, and the dihedral angle measured.

A number of micrographs were taken to record some of the interesting phenomena in the structure of the thermally

etched nickel.

Difficulties.

Temperature measurement and control.

Temperature measurement inside the experimental zone, and temperature control were subject to considerable difficulties. In the first test when the platinum thermocouples were introduced into the nickel box, it was observed that they became contaminated with condensed nickel vapor, making the readings completely unreliable. In the attempts which followed, the thermocouples had to be removed from the actual experimental zone and covered with suitable shielding material, thus introducing uncertainty in the experimental temperature. The magnesium silicate (AlSiMag 222) tube which served as the support for the nickel box containing the specimens, was found to be satisfactory. Metal shields, such as titanium and molybdenum, were entirely unsatisfactory because of their tendency to form alloys with condensing nickel, and to melt around the thermocouple.

The thermocouples were observed to pick up an induced A.C. voltage of up to 70 volts from the furnace winding during the experiments at high temperatures. To correct the situation, thermocouples inserted in the magnesium silicate support were shielded with grounded molybdenum sheets. This method decreased the A.C. voltage in the thermocouple to less than 1 volt, but the other thermocouple used for control purposes and situated outside the furnace winding was never free from an A.C. voltage of at least about 15 volts.

Temperature gradient.

During the production of thermally etched nickel metallographic specimens, as well as the thermal treatment of nickel wires to determine the surface tension of the metal, the presence of a considerable temperature gradient inside the furnace was observed. Although the effect of this gradient would be somewhat diminished by the high thermal conductivity of nickel, its undesirable effects on the experimental specimens were easily detectable. Metallographic specimens prepared for interferometric technique to determine the grain boundary energy of solid nickel were found to be unsatisfactory because of the sublimation of nickel atoms on the polished surfaces. The original wire size was increased up to 50 percent of its original diameter because of the condensation of nickel vapour in the cooler regions of the hot zone, and partially decreased at the hotter spots. Furthermore, the weights suspended on the wires were found to have increased up to 50 percent with respect to the originally determined loads for the same reason. To improve the thermal gradient in the furnace the following corrective steps were taken: the original gage length of the wires, which was approximately 8 centimeters, was decreased to about 2 centimeters; more radiation shields were introduced, and the heating coil re-designed. Considerable improvement was observed. however, there was still some indication of a thermal gradient in spite of this, the nickel box appeared to lie in a region of reasonably uniform temperature.

High vapour pressure of nickel.

To decrease the high rate of evaporation of nickel atoms at elevated temperatures, it was decided to use inert gas atmospheres instead of vacuum. A helium atmosphere of 760 mm Hg was found to be unsatisfactory because of its very high thermal conductivity, the maximum temperature reached staying below 1200°C. An argon atmosphere of 760 mm Hg was used successfully, the maximum attainable temperature approaching 1400°C.

The structure of experimental wires.

The fine wires employed employed in the force measurement technique to determine the surface tension of solid nickel were two to three times greater in diameter than those used by other workers on copper, gold, and silver. In the previous work the reported diameters of the wires used were 0.003 and 0.005 inches compared to 0.010 inches in the present case. The use of finer wires is considered to be a factor in securing a satisfactory bamboo-like structure of the wires during the experimental tests. As a consequence, an ideal bamboo-like structure of the wires was seldom observed after experimental runs. Furthermore, much longer durations of the experimental runs had to be applied to achieve measurable strains.

Interferometric work

After many unsuccessful attempts to observe the Fizeau fringes according to the method described previously, optical immersion oil was employed between the specimen and

Fig. 8 Vacuum Furnace with Control Instruments

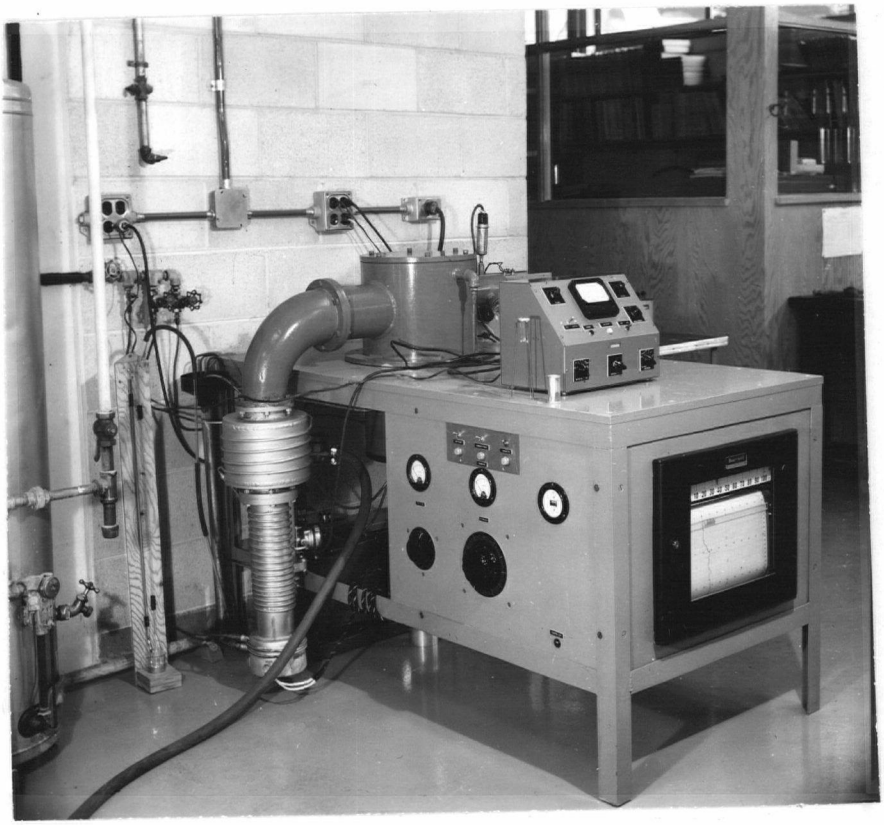

Fig. 9 Vacuum Furnace with Control Instruments

the coated slip, as proposed by Hilliard. No fringes were detected in the regions where oil was squeezed between the specimen and the glass plate, but they were clearly visible in the regions where no oil was present. It is assumed that this thin layer of oil carrying the weight of the specimen promotes an almost perfect parallelism between the thermally etched surface and the reference plate.

IV. RESULTS

The Grain Boundary Energy of Solid Nickel.

The relative grain boundary energy of solid nickel was determined by measuring the dihedral grain boundary groove angle of thermally etched commercially pure nickel specimens. The interferometric method as proposed by Hilliard and Harrold was used.

Matching an aluminized optically flat glass surface of reflectivity approximately 0.30, against the thermally etched specimen, and using monochromatic light (Hg green line of 5461 Angstroms), Fizeau fringes representing the contour lines in the surface topography were observed and photographed at a magnification of 1170 times. Distances between the respective Fizeau fringes were measured to 0.005 cm by using a microscope. Knowing the magnification of the micrograph, the horizontal distances between the Fizeau fringes were calculated and plotted against the constant vertical distances between the fringes, which were equal to $\lambda/2$ or to 2.7305×10^{-5} cms. From

the resulting elevation profile of the surface slope in the grain boundary groove, the dihedral angle Ψ was measured.

A few of the micrographs (Figures 10, 11, 12, and 13) showing the Fizeau fringes along the grain boundaries of thermally etched nickel specimens, and the determination of dihedral angles from those are presented on pages 36 and 37.

Table I gives the horizontal distances between the fringes, measured at the cross-sections as indicated on the micrographs, and calculated, taking into account the magnification.

Fig. 14 shows one of the elevation profiles of the grain boundary groove plotted from the attained interferometric data.

The tests to produce thermally etched specimens of four hours duration were carried out in vacuum of 5×10^{-5} mm Hg at 1375°C. Because of the experimental difficulties, only three different grain boundaries have been studied interferometrically.

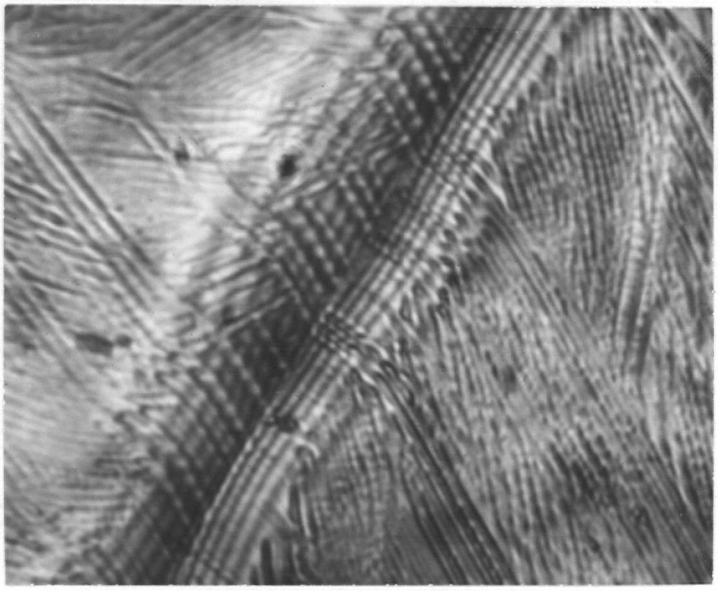

Fig. 10 1100x

Micrograph Showing the Fizeau Fringes along the Grain Boundary of a Thermally Etched Nickel Specimen.

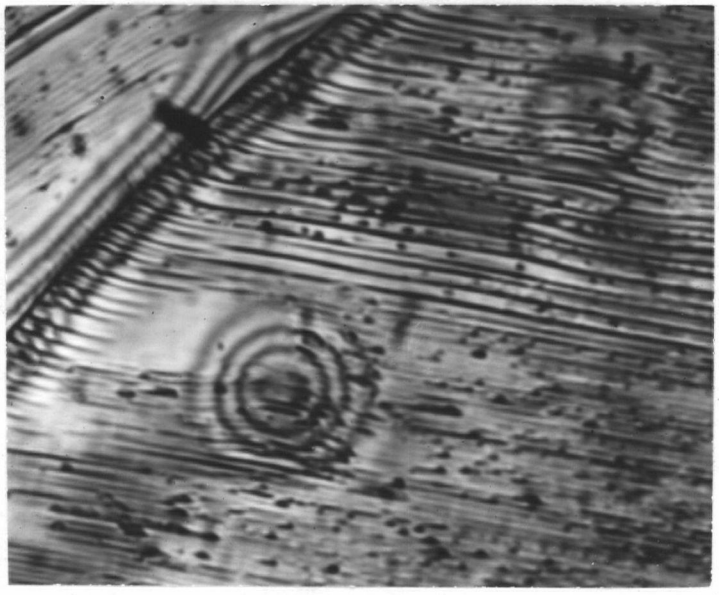

Fig. 11 1100x

Micrograph Showing the Fizeau Fringes.

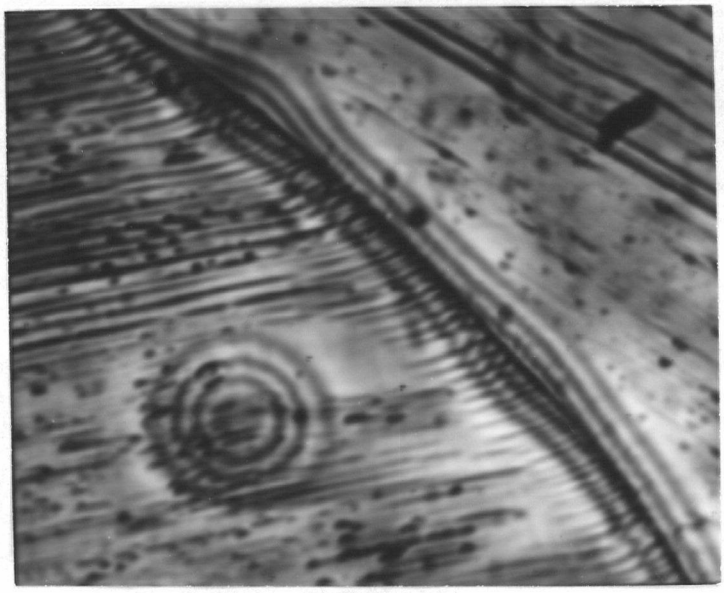

Fig. 12 1100 x

Micrograph Showing the Fizeau Fringes.

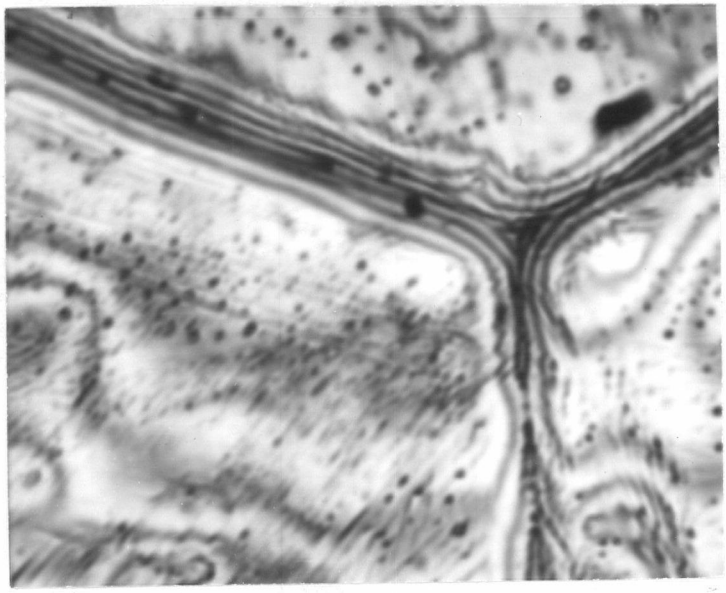

Fig. 13 1100 x

Micrograph Showing the Fizeau Fringes.

TABLE I

Horizontal Distances Between the Fizeau Fringes Measured from the Experimental Micrographs.

Profile									
1		2		3		4		5	
a*	b*	a*	b*	a*	b*	a*	b*	a*	b*
0.205	17.5	0.190	16.3						
0.195	16.7	0.160	13.7						
0.190	16.3	0.155	13.2	0.250	21.4	0.275	23.5	0.190	16.3
0.170	14.6	0.145	12.4	0.220	18.8	0.240	20.5	0.180	15.4
0	0	0	0	0	0	0	0	0	0
0.175	15.0	0.160	13.7	0.230	19.7	0.260	22.0	0.175	15.0
0.205	17.5	0.185	15.8	0.260	22.2	0.300	25.5	0.210	18.0
0.215	18.4	0.215	18.4						
0.265	22.7	0.245	21.0						

* a gives the measured distance between fringes in cm.

* b gives the calculated real distances between fringes in 10^{-5}cm.

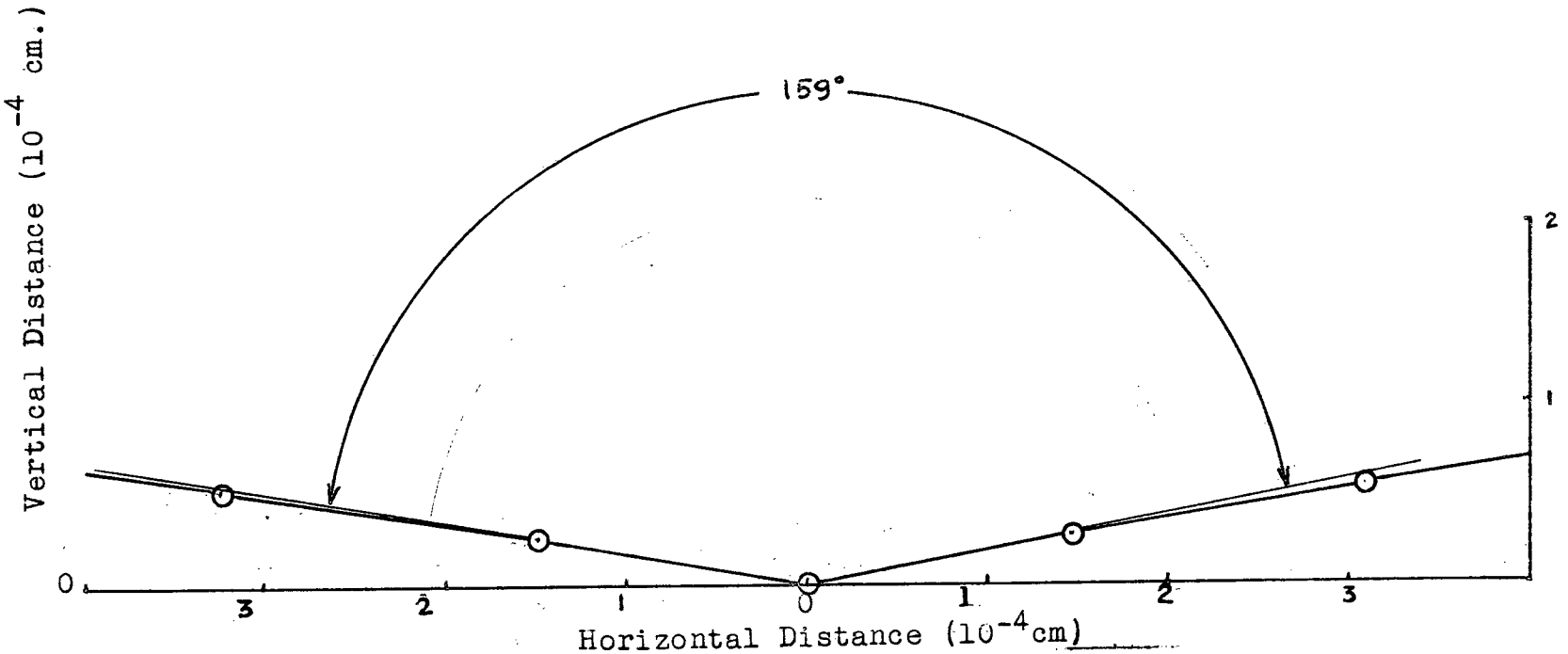

Fig. 14 Elevation Profile No. 1 of the Grain Boundary Groove Plotted from the Interferometric Data.

The values of dihedral angles determined from the above data are recorded in Table II.

Table II

Values of Dihedral Grain Boundary Angles of Thermally Etched Commercially Pure Nickel.

Profile	Dihedral Angle ψ	$\frac{\psi}{2}$	$\cos \frac{\psi}{2}$	$\frac{\gamma^*}{\gamma}$
1	159	79.5	0.182	0.364
2	156	78	0.208	0.416
3	164	82	0.139	0.278
4	165	82.5	0.131	0.262
5	159	79.5	0.182	0.364

The scattering of the values obtained for the dihedral angle causes, as seen from the above table, a variation of the ratio γ^*/γ up to ± 30 percent with respect to the average value, 0.33. This large variation cannot be explained by the orientation dependence of the grain boundary energies. It is expected that the average grain boundary lies between grains so different in orientation that the dihedral angle would be virtually constant. Hence, the reason for the scatter most probably lies in the experimental technique or conditions. It is not believed that Hilliard's interferometric method has inherently low precision, rather, in the present case the scatter results from two contributing factors. First, the very shallow nature of the grain boundaries revealed in the specimens, i.e., only two to four fringes in depth did not permit the accurate plotting of profile. Hilliard, however,

was able to get boundaries six to eight fringes in depth and so was able to draw better and more accurate profiles. Secondly, only a very few boundaries were found where fringes could be observed, whereas,ideally,a fairly large number would be necessary in order to get truly representative values.

An attempt was made to measure the dihedral grain boundary groove angles of thermally etched nickel in micro-sections taken perpendicular to the surface. The thermally etched grain boundaries of the specimen were observed in profile and the suitable ones were photographed at a magnification of 1100 times. The region containing the grain boundary groove was magnified (Fig. 15) from the prints and the dihedral angle measured. According to this method the dihedral angle was found to be equal to 146 degrees.

As stated on the previous pages (page 17), the interferometric method is considered to be more accurate than the microsectional one because of its relative simplicity and involvement of fewer experimental uncertainties. Hence, in the following calculations, despite its uncertainty because of the small number of experimental determinations, an average value of 161 degrees is used to determine the relative grain boundary tension of solid nickel according to the equation

$$\gamma^{*} = 2\gamma \cos \frac{\Psi}{2}$$

From this equation the ratio of grain boundary energy to surface tension for solid nickel was found to be approximately 0.33 for the average value of dihedral angle. This ratio has

been proposed and confirmed for copper, gold, and silver.

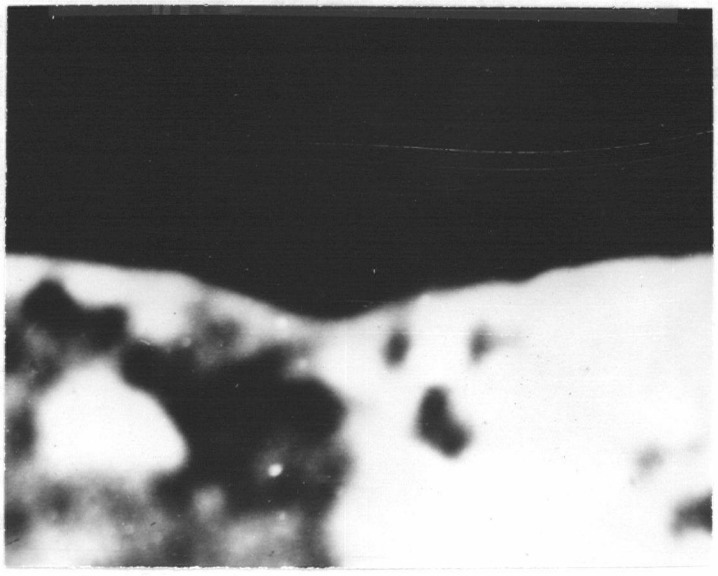

Fig. 15 Micrograph Showing the Microsection of Grain Boundary of Thermally Etched Nickel at 1375°C for 4 Hours. Original Magnification 1100x, enlarged 8x.

The Surface Tension of Solid Nickel

Strain and stress measurements within the recorded temperature range for a determined length of time are given in Table III. The atmosphereic conditions of the successful experiments are also indicated.

These results are plotted graphically in a stress-strain diagram, to determine the load which exactly balances the upward pull of the surface tension. Figure 16 is a typical plot. Actually the value for stress at zero strain, as well as the slope, was calculated by using the method of least squares.

Table IV gives the values of surface tension and grain boundary energy determined from the stress at zero

Table III

Experimental Stress and Strain Measurements.

Test No.	1		2		4	
Temp. °C.	1300±5		1300±5		1391±5	
Time hours	20		70		19	
Atm. mm Hg	5×10^{-5}		5×10^{-5}		5×10^{-5}	
Wire radius cm.	0.01425		0.0129		0.0127	
Spec. No.	Stress dyne/cm^2 x 10^{-5}	Strain cm/cm x 10^3	Stress dyne/cm^2 x 10^{-5}	Strain cm/cm x 10^3	Stress dyne/cm^2 x 10^{-5}	Strain cm/cm x 10^3
1	1.75	-2.43	0.568	-6.15		
2	3.23	-1.61	1.065	-3.18	2.56	-5.77
3	4.07	0.328			3.75	-6.45
4			1.44	-2.71	4.30	-4.05
5			1.91	-1.01	5.77	-1.88
6					6.40	-0.405
7			4.26	-0.29		
8			5.41	1.00		

Test No.	6		7		10	
Temp. °C	1395±5		1350±5		1375±5	
Time hours	20		50		50	
Atm. mm Hg	5×10^{-5}		5×10^{-5}		5×10^{-5}	
Wire radius cm.	0.0127		0.0127		0.0127	
Spec. No.	Stress dyne/cm x 10^{-5}	Strain cm/cm x 10^3	Stress dyne/cm x 10^{-5}	Strain cm/cm x 10^3	Stress dyne/cm x 10^{-5}	Strain cm/cm x 10^3
1	2.09	-6.02	2.37	-0.774	0.92	-0.70
2	3.92	-4.93	4.36	-0.543		
3			6.02	-0.056	2.21	-0.115
4			7.97	0.728	4.04	0.97
5	9.61	1.46	10.82	1.32	5.42	1.73
6			12.27	1.94	5.50	1.98
7			13.67	1.79	7.46	3.41
8						

TABLE III (cont'd.)

Test No.	11		12		13	
Temp. °C	1327±10		1300±10		1380±10	
Time hours	75		96		6	
Atm. mm Hg	760 (Argon)		760 (Argon)		760 (Argon)	
Wire radius cm.	0.0123		0.0127		0.0126	
Spec. No.	Stress dyne/cm^2 x 10^{-5}	Strain cm/cm x 10^3	Stress dyne/cm^2 x 10^{-5}	Strain cm/cm x 10^3	Stress dyne/cm^2 x 10^{-5}	Strain cm/cm x 10^3
1	0.749	-1.005				
2	0.949	-0.843				
3	1.58	0.076	1.44	-1.38	1.52	0.115
4	2.65	0.527	2.92	-0.46	2.52	0.972
5	4.06	1.006	3.71	1.087	3.87	1.732
6			4.01	1.087	4.18	1.977
7			5.54	1.55		

Test No.	14		15	
Temp. °C.	1380±10		1366±10	
Time hours	24		70	
Atm. mm Hg	760 (Argon)		760 (Argon	
Wire radius cm.	0.0126		0.0117	
Spec. No.	Stress dyne/cm^2 x 10^{-5}	Strain cm/cm. x 10^3	Stress dyne/cm^2 x 10^{-5}	Strain cm/cm. x 10^3
1	0.728	-1.32	0.836	-1.22
2	0.950	-0.19	1.05	-0.55
3	1.525	0.382	1.76	0.207
4	2.52	1.79	2.98	0.738
5				
6			4.87	1.68
7			6.73	2.14

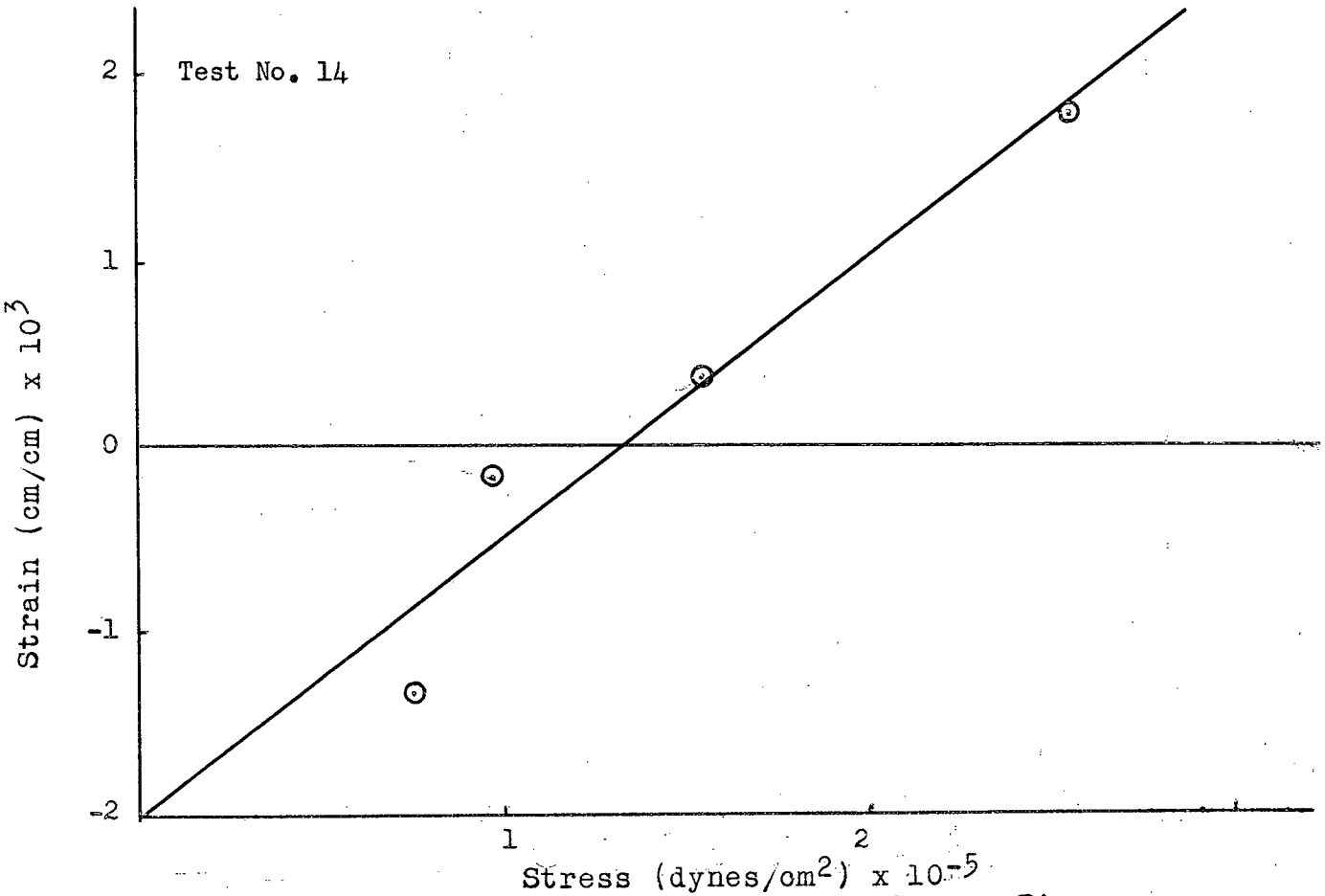

Fig. 16 A Typical Experimental Stress-Stress Diagram.

TABLE IV

Experimental Values of the Surface Tension and Grain Boundary Energies of Solid Nickel.

Test No.	Atmos.	Temp. °C.	Duration of test hours.	$\sigma_{\epsilon=o}$ dyne/cm^2 10^{-5}	Surface Tension dyne/cm	Grain Bound. Energy dyne/cm.
1	Vacuum	1300±5	42	4.07	6760	2253
2	Vacuum	1300±5	79	4.22	6370	2123
4	Vacuum	1391±5	19	6.97	10320	3440
6	Vacuum	1395±5	20	8.30	12300	4100
7	Vacuum	1390±5	50	6.71	11130	3710
10	Vacuum	1375±5	50	2.50	44160	1387
11	Argon	1327±10	75	2.08	2990	997
12	Argon	1300±10	96	2.95	4410	1470
13	Argon	1380±10	6	1.67	2470	823
14	Argon	1380±10	24	1.33	1970	657
15	Argon	1366±10	70	2.16	2920	973

strain, by use of the two simultaneous linear equations,

$$w = \pi r \gamma - \left(\frac{n}{\ell}\right) \pi r^2 \gamma^*$$

$$\gamma^* = 2\gamma \cos \frac{\Psi}{2}$$

where, as before

w = suspended weight

γ = surface tension

γ^* = grain boundary energy

r = radius of the wire

$\frac{n}{\ell}$ = number of grains per unit length.

The value for n/l, the number of grains per unit length of the wire, was determined after every run by cutting pieces of the nickel wire specimens, 1 cm. long, and mounting in lucite, polishing, etching, and observing these specimens under the microscope. The number of grains per cm of wire was determined to be 30±10. A characteristic micrograph demonstrating the structure of the nickel wire is given in Figure 17 where the so-called 'bamboo-like' structure can be observed.

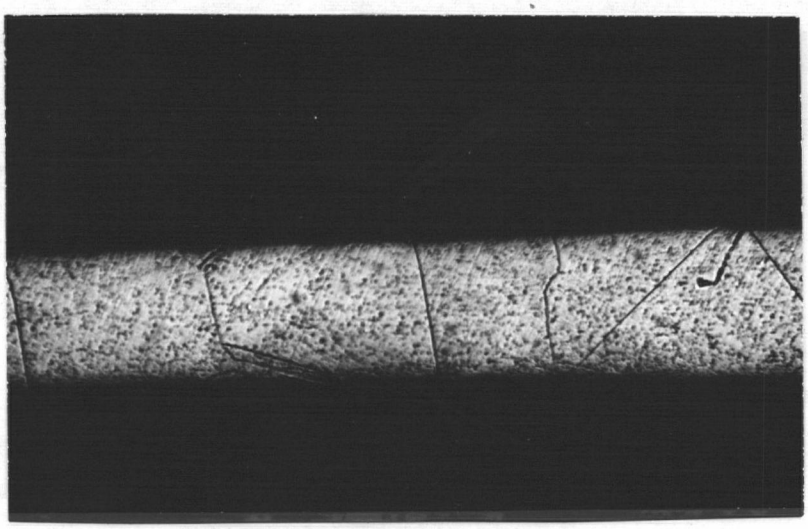

Fig. 17 250x

Micrograph Showing the 'Bamboo-like' Structure of Experimental Wires.

V. DISCUSSION

Surface Energy Measurements.

The value of the dihedral grain boundary groove angle for thermally etched nickel was found to be 161 degrees according to the interferometric method. On the basis of the present work and as described earlier the accuracy of this method is believed to be higher than that of other conventional techniques. Furthermore, the interferometric method in comparison with the microsectional one was found to be simpler because of the relative ease in picking visually the grain boundary grooves suitable for the measurement of dihedral angle by observing the symmetry of the Fizeau fringes. Hence, the above value for the dihedral grain boundary groove angle of thermally etched nickel is thought to be acceptable although, of course, no attempt has been made to account for the orientation dependence of the grain boundary angle. Furthermore, this value cannot be taken as final because of the small number of tests carried out successfully.

Substituting the determined value of the dihedral angle in the equation

$$\gamma^* = 2\gamma \cos \frac{\psi}{2}$$

gives the ratio of grain boundary tension over surface tension for solid nickel. This ratio was determined to be approximately 0.33 which checks very well with the assumption for nickel. Similar values had been postulated and confirmed experimentally for copper, gold, and silver.

The surface tension of solid nickel determined in a vacuum of 5×10^{-5} mm Hg in the temperature range from 1300°C to 1395°C was found to vary inconsistently from 4160 to 12,320 dynes per centimeter. The combination of the high vapour pressure of nickel under these experimental conditions, and the sharp thermal gradients within the hot zone, results in excessive evaporation from some parts of the system and condensation onto other parts of the system. This produces changes in the dimensions and weights of the test components. Therefore, little reliance may be placed in the results obtained from tests in vacuum.

To overcome the difficulties due to the high vapour pressure of nickel, an inert gas atmosphere was employed in the experiments. The surface tension of solid nickel in argon at 760 mm Hg in the temperature range from 1300°C to 1380°C was determined to vary from 1970 to 4410 dynes per centimeter. The lower values, 1970 and 2470 dynes/cm are thought to be most reliable.

It will be seen that of the runs made with an argon atmosphere, those made with the longest times have the greatest surface tension value. The time factor may be coincidental, since the microstructures of the wires giving the larger values were not bamboo-like, and for this reason alone these values can be rejected.

However, since the vacuum runs are all high, it may be that evaporation is partly to blame. It should be noted that the argon atmosphere does not prevent the evaporation of nickel, it merely reduces the partial pressure of nickel so that evaporation

is diminished. The vapour pressure of nickel at 1357°C is in the order 10^{-3} mm.

A recent paper by Skapski[46] enables a calculation of surface tension to be made if certain values are known. Appendix E shows the calculation for nickel. It was necessary to extrapolate data by Norton[58] in order to get a value for the surface tension of liquid nickel at the melting point since the capillary coefficient of liquid nickel is unknown.

Table V.

Calculated Values of the Surface Tension for Solid Nickel (dynes/cm).

σ_L	$\sigma_{s\ M.P}$	$\sigma_{s\ 1380°C}$
1450	1630	1671
1500	1680	1721
1550	1730	1771
1600	1781	1822
1650	1831	1872
1700	1882	1923

The above table gives the calculated values and it will be seen that they agree in order of magnitude with the observed surface tensions.

It is instructive to compare the results of Skapski as in Table VI.

Table VI

Metal	$\sigma_{s\ calc}$	$\sigma_{s\ obs}$
Ag	1056	1130±60
Au	1267	1350±70
Cu	1417	1650±80

All the calculated values are less than the observed ones, but the theory gives good general agreement and supports the choice of the two lowest observed values, and their arithmetical average is henceforth used. The precision of the final value is difficult to assess but is probably better than 300 dynes/cm. Hence, it is proposed on the basis of the present work that the surface tension of solid nickel in argon within the temperature range from 1370°C to 1390°C is 2220±300 dynes per centimeter.

Thus the grain boundary energy of solid nickel within the previously stated experimental conditions would be 740±300 dynes per centimeter.

However, these values cannot be considered as final and conclusive because of the small number of tests carried out successfully under satisfactory experimental conditions. Nevertheless, it is believed that these values can be confirmed in future tests provided that the temperature control in the experimental zone is sufficiently close, the temperature gradient is negligible, and the structure of the experimental wires approaches the so-called 'bamboo-like' structure. A finer wire size, 0.003 to 0.005 inches diameter, would be desirable.

It had been hoped that the value for the temperature coefficient of the surface tension of solid nickel, and the value for the viscosity of solid nickel could be established experimentally, but the idea had to be abandoned because of the shortness of time and the insufficiently close control of temperature during the tests.

Thermal Etching.

During the experimental work to determine the grain boundary energies of solid nickel, the structures of the thermally etched metallographic specimens were examined for evidence indicating the presence of dislocations.

The dislocation concept has been found to be useful in explaining crystal structure, diffusion, solidification, and deformation, but until lately direct experimental observations have been scarce. According to Forty[48] very little work has been done on metals, most of the observations being carried out on non-metals.

From the calculations based on a dislocation model of a small-angle grain boundary, it is expected that the spacing of individual dislocations along such a boundary is within the resolving power of the optical microscope.[49-53] Hence, it is conceivable that a microscope of sufficiently high magnification power would reveal the dislocations.

The dislocations in low-angle boundaries as well as in the matrix can be revealed with methods based on the assumption that a dislocation is a structural discontinuity causing energy-difference in the crystal lattice. The most useful method to reveal the dislocations is the sensitive etching, which may be accomplished by chemical, electrochemical, ionic bombardment, or by thermal etching. All these techniques involve the removal of atoms from the high-energy dislocation sites, the rate of migration from these sites being higher than from the neighboring

matrix.

This method has been employed to show the presence of dislocations in silver[54] and in chromium.[55]

Commercially pure nickel thermally etched at 1350°C and at a pressure of 5×10^{-5} mm Hg for four hours showed the following structure (Figs. 18-27).

The existence of dislocations in chromium[55] had been concluded from the following features revealed after a suitable thermal etch:

1. The existence of sub-boundaries developed as rows of pits.

2. The occurrence of generally spaced pits within the sub-grain.

3. The dihedral angles between sub-boundaries themselves and between the sub-boundaries and the grain boundaries.

In the present work no sub-boundaries were detected as rows of etch pits, Figs. 18 and 19 , however, show sub-boundaries but not as a row of pits. The continuous solid boundary could be considered as a sub-boundary since the degree of mismatch across the boundary is very small. The absence of rows of etch pits might be due to the decreased sensitivity of the thermal etch at the higher temperatures as in the work on chromium.

Similarly, the occurrence of generally spaced pits

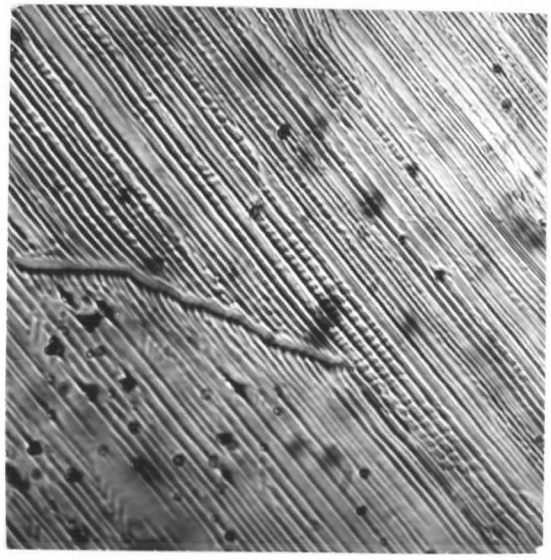

Fig. 18 1100 x

Thermally Etched Nickel Specimen Showing a Sub-boundary.

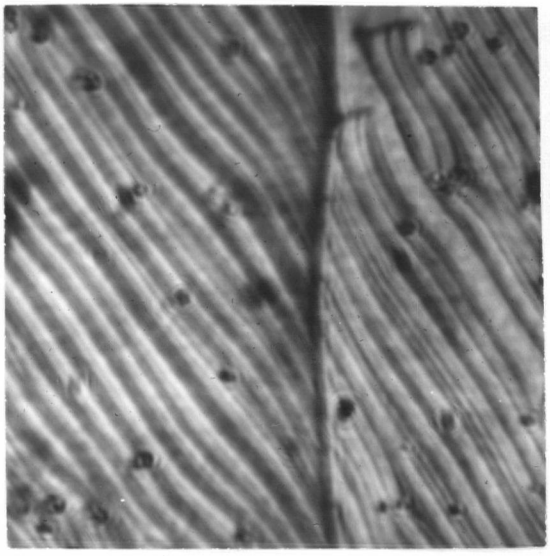

Fig. 19 2300 x

Thermally Etched Nickel Specimen Showing a Sub-boundary.

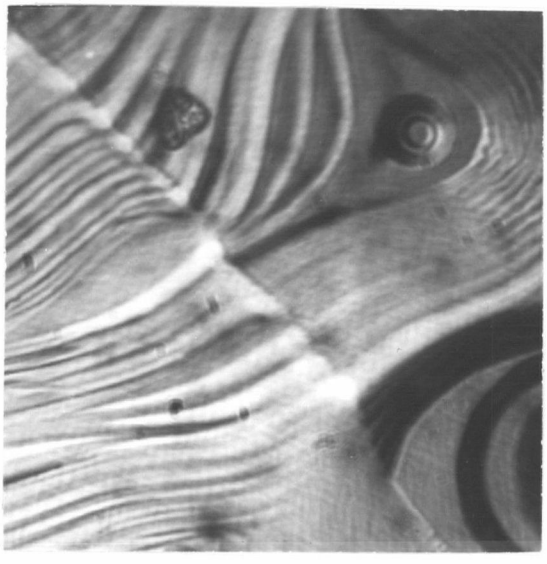

Fig. 20 2300 x

Thermally Etched Nickel Specimen Showing the Configuration around an Inclusion.

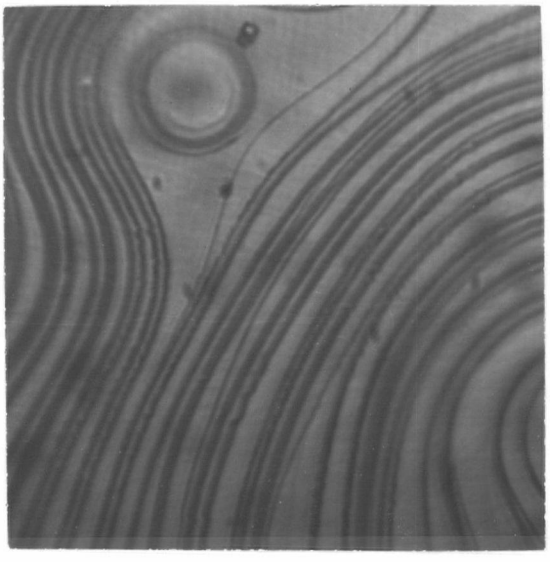

Fig. 21 2300 x

Thermally Etched Nickel Specimen Showing the Configuration around an Inclusion.

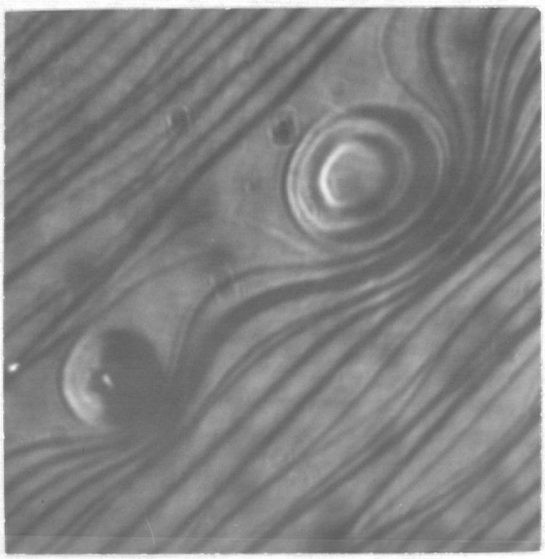

Fig. 22 2300 x

Thermally Etched Nickel Specimen Showing the Configuration around Two Inclusions.

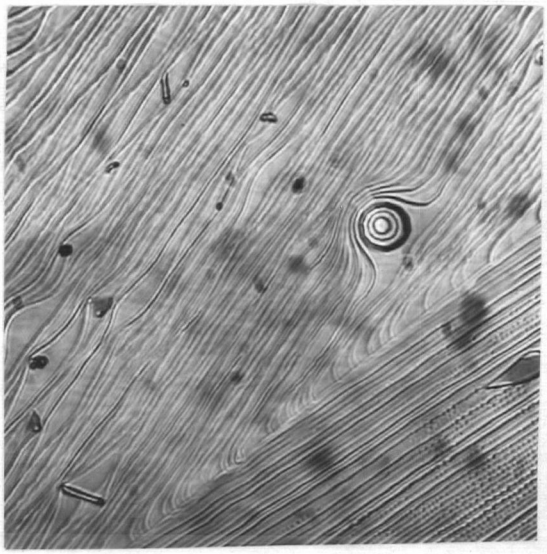

Fig. 23 550 x

Thermally Etched Nickel Specimen Showing a Symmetrical Deep Pit.

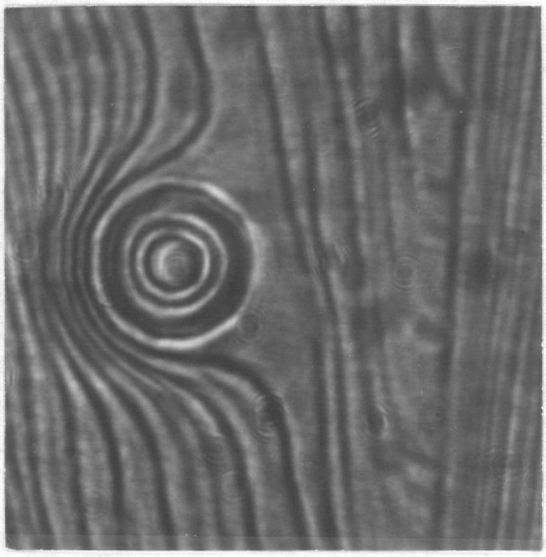

Fig. 24 2300 x

Thermally Etched Nickel Specimen Showing the Symmetrical Deep Pit from the Fig. 23.

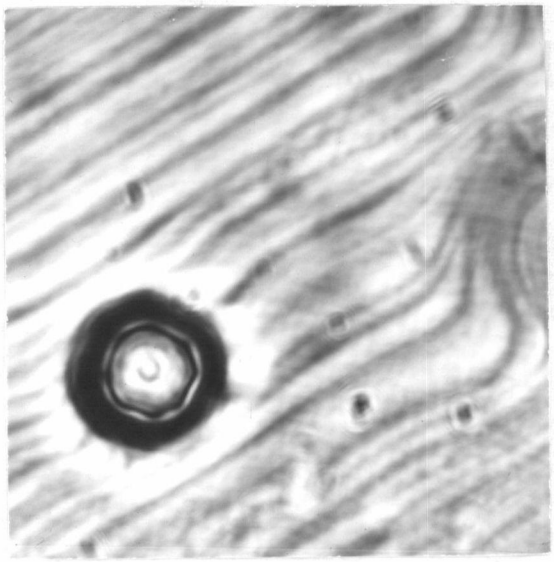

Fig. 25 2300 x

Thermally Etched Nickel Specimen Showing an Octahedral Deep Pit.

Fig. 26 1100 x

Thermally Etched Nickel Specimen Showing some Symmetrical Features.

Fig. 27 1100 x

Thermally Etched Nickel, Chemically Etched before Thermal Treatment.

within the grains was dubious. However, interesting configurations around the inclusions were noted in the metallographic study of thermally etched nickel. Such patterns around an inclusion are demonstrated in Figures 20, 21 and 22.

Figures 23 to 25 show the structures similar to those noted in the chromium etched at higher temperatures only (1500°C). The relatively deep pit, shown in Figure 25, exhibits octagonal symmetry at its base. The inclusion of Figure 23 magnified in Figure 24 shows hexagonal symmetry at its base and dodecahedral in the second and third levels from the base. It has been postulated that this symbolizes the reverse process of spiral growth as proposed by Frank[56] and directly observed in cadmium iodide crystals by Newkirk. Thus, screw dislocations may be operative in permitting sublimation to take place at temperatures at which the vapour pressure corresponds to low supersaturations. Danko and Griest[57] observed similar sublimation figures on the surface of pure nickel, copper, and zinc specimens. They found that the geometry of the sublimation figure of nickel and zinc corresponded to their respective crystal structures, the figures on the copper specimens being of circular nature. In the course of the present work no cubic sublimation figures were observed on the thermally etched nickel specimens, as reported by Danko and Griest. However, triangular, hexagonal, and circular configurations were exhibited in some cases (Fig.26). The specimen seen in the Figure 27 was chemically etched prior to the thermal treatment.

VI. CONCLUSIONS

1. The surface tension of solid nickel in argon at 760 mm Hg and within the temperature range from 1370°C to 1390°C was determined to be 2220±300 dynes per centimeter.

2. The grain boundary energy of solid nickel in argon within the previously stated temperature range was found to be 740±300 dynes per centimeter, assuming the ratio of grain boundary energy to surface tension for nickel to be 1/3.

3. The dihedral grain boundary groove angle of thermally etched solid nickel was determined interferometrically and measured to be 161 degrees.

4. The ratio of grain boundary energy to surface tension for solid nickel, using the measured dihedral angle, was calculated to be approximately 0.33 which checks well with the assumption of 1/3.

5. The physical evidence for dislocations in nickel was inconclusive on the basis of observations on the structures of the thermally etched nickel specimens in vacuum of 5×10^{-5} mm Hg and at 1350°C. Nevertheless, a more sensitive thermal etch at lower temperatures is expected to produce more convincing physical evidence of dislocations in nickel.

6. Udin's technique to determine the surface tension of metals by force measurement on stretched wires was found to be satisfactory on a metal of higher melting point, provided

precautions were taken to reduce the high vapour pressure of the metal.

7. Hilliard's interferometric method to measure the dihedral grain boundary groove angles was found to be applicable and simple. The accuracy of the method was not very high in the present work, but this could be blamed on the small number of tests carried out. It is believed that the precision of this method is not inherently low.

VII. APPENDICES

APPENDIX A

DEFINITIONS

Interface

An interface is defined to be a bounding surface across which a discontinuity can be observed.

Grain boundary

In the solid state the observed interfaces due to a discontinuity may be caused by different changes. If the interface is due to a sudden change in lattice orientation within a single phase, it is called a grain boundary.

Interfacial energy

Atoms in the discontinuous regions or interfaces do not have their normal number of neighbors at normal distances, they are in higher energy states compared to the atoms in neighboring homogeneous regions. The total excess energy of these interfacial atoms due to the abnormal structural arrangement, is called interfacial energy.

Grain boundary energy

Grain boundary energy is the excess energy of the interfacial atoms due to the abnormal crystallographic arrangement.

Specific interfacial energy

The specific interfacial free energy may be defined as the increase of free energy of a system per unit increase of interfacial area under conditions so that the new interface has its minimum energy configuration.

Interfacial force

The fictitious force per unit length which is assumed to replace the free energy per unit area of interface in calculations has the same physical dimensions and is considered to be a tension as the interfacial energies are always positive.

Surface tension.

The surface tension is defined to be the interfacial force, if a solid or liquid is in equilibrium with the vapour in a vacuum or in a noble gas atmosphere.

APPENDIX B

Nominal Composition of Commercially Pure Nickel of Type "A" Grade

Ni (Co)	Fe	Mn	Cu	C	Si	S
99.4%	0.15%	0.20%	0.10%	0.10%	0.05%	0.005%

Electrical Power Supply, Thermocouple, and Vacuum Gauge Circuits.

A - Ammeter
L - Lamp
R - Relay
P - Potentiometer
S - Specimen
T - Time elapse meter

V.G. - Vacuum gauge control
I.G. - Ionization gauge
T.C.G. - Thermocouple gauge
T.C. - Thermocouple
C.J. - Cold junction
D.P. - Diffusion pump

M.P. - Mechanical pump
R.C. - Recorder-controller

APPENDIX D

Preparation of 50 Percent Transmittent Mirrors.

Determination of the thickness of the film for 50 percent transmission.

Formulas:

$$x_{\frac{1}{2}} = \frac{0.693}{\mu} \qquad \mu = \frac{4\pi nk}{\lambda}$$

Data:

	Absorption index k	Refractive index n	nk for green Hg spectral line of 5461 A
Silver	17.9	0.175	3.30
Aluminum	3.48	1.16	4.04

Calculation:

$$\mu = \frac{4(3.14)(4.04)}{5461 \times 10^{-8}} = 0.928 \times 10^{6} \text{ cm}^{-1}$$

$$x_{\frac{1}{2}} = \frac{0.693}{0.928 \times 10^{6}} = 0.747 \times 10^{-6} \text{ cm}$$

Determination of the weight of metal needed for 50 percent transmission to coat the glass.

Formula:

$$x_{\frac{1}{2}} = \frac{m}{4\pi\rho r^2}$$

where ρ is the density of the metal.

r is the distance between source of coating metal and glass

m is the weight of metal needed

Data: r is 15 cm.

	Density	Thickness of Film $x_{\frac{1}{2}}$
Silver	10.5	0.911×10^{-6} cm
Aluminum	2.7	0.747×10^{-6} cm

Calculation: $m_{Al} = 4(3.14)(2.7)(15^2)(0.747 \times 10^{-6}) = 27$ mg.

APPENDIX E

Calculation of the Surface Tension of Solid Nickel

According to Skapski[53] the surface tension of metals can be calculated from the arrangement of their next-neighbors, from the heat of fusion, and from the surface tension of the liquid at the melting point. The following equation:

$$\sigma_s = \frac{Z_o}{Z_i}\frac{Q_f}{A_s} + \left(\frac{\rho_s}{\rho_l}\right)^{\frac{2}{3}}\sigma_L + \frac{1}{2}\frac{T_m}{A_s}\left[\Delta S_{L\,conf} - \Delta S_{s\,conf}\right] \qquad (1)$$

holds for the calculation of the surface tension of a solid in its most densely populated planes to reveal the minimum surface tension, where

Z_a = number of next-neighbors on the surface

Z_i = number of next-neighbors in the lattice.

$Z_o = Z_i - Z_a$

Q_f = heat of fusion

ρ_s = density of solid at melting point.

ρ_L = density of liquid at melting point

σ_L = specific surface tension of liquid

T_m = melting point in ^oK

$\Delta S_{L\,conf}$ = configurational entropy for the liquid surface.

$\Delta S_{s\,conf}$ = configurational entropy for the solid surface.

A_s = molar area.

$$A_s = f N^{\frac{1}{3}}\left(\frac{M}{\rho_s}\right)^{\frac{2}{3}}$$

where

f = density factor

N = Avogadro's number

M = molecular weight

$$\sigma_L = \frac{X^2}{4}\rho_L g$$

where

g = gravity acceleration

X = height of the lower surface of the plate above the undisturbed level of the liquid.

Following Skapski, for nickel, which is a face-centred cubic metal, the minimum surface tension can be calculated in the most densely populated planes, 111-planes.

For nickel:

$Z_i = 12$

$Z_a = 9$

$Z_o = 12 - 9 \quad 3$

$\frac{Z_o}{Z_i} = 3/12 = 1/4$

$f = 1.09$

$M = 58.69$

$T_m = 1455^{\circ}C.$

$\Delta S_{L\,conf} = 4.48 \times 10^7$ ergs/degree

$\Delta S_{s\,conf} = 3.90 \times 10^7$ ergs/degree

$Q_f = 18.18 \times 10^{10}$ ergs/gram-atom (Metals Handbook)

ρ_s is calculated from the lattice parameter of nickel.

$a = 3.517 \times 10^{-8}$ cm, and from the cubical thermal expansion coefficient;-

$\beta = 38.1 \times 10^{-6}$ cm/m, according to Mott and Johnson[59]

$$a^3_{1455^{\circ}C} = (3.517 \times 10^{-8})^3(1 + 3.81 \times 10^{-6}(1455-20))$$

$$a^3_{1455^{\circ}C} = 46 \times 10^{-24}\ cm^3$$

$$\rho_{s\ 1455^{\circ}C} = \frac{4(58.69)}{6.0235 \times 10^{23}(46 \times 10^{-24})} = 8.48\ g/cm^3$$

Since no data is available concerning the density of liquid nickel at the melting point, the decrease in density of solid nickel at the same temperature is assumed to be similar to that of copper. Hence, the density of liquid nickel at the melting point is taken to be equal to 8.26 g/cm.[3]

$$\rho_L = 8.26 \text{ g/cm}^3$$

From equation (2)

$$A_S = 1.09(6.0235\times10^{23})^{\frac{1}{3}}(58.69)^{\frac{2}{3}} = 33.4\times10^7 \text{ cm}^2$$

Because the capillary constant for liquid nickel is unknown, the values of σ_L has been extrapolated from the data presented by Norton et al.[58] Owing to the uncertainty of this extrapolation, calculations were made for six different values of σ_L and results are presented below:

From equation (1)

$$\sigma_{S_{M.P}} = \frac{1}{4}\left(\frac{18.18\times10^{10}}{33.4\times10^7}\right) + \left(\frac{8.48}{8.26}\right)^{\frac{2}{3}}(1550) + \frac{1455+273}{2(33.4\times10^7)}(4.48-3.90)\times10^7$$

$$= 136 + 1.018(1550) + 2.59(0.58)$$

$$= 136 + 1579 + 15$$

$$\sigma_{S_{M.P}} = 1730 \text{ dynes/cm at } 1455^\circ\text{C}.$$

Assuming the thermal coefficient for surface tension of solid nickel be equal to that of solid copper, 0.55 dynes/cm/°C

$$\sigma_{S_{1380^\circ C}} = 1730 + 0.55(1455 - 1380)$$

$$= 1730 + 41$$

$$\sigma_{S_{1380^\circ C}} = 1771 \text{ dynes/cm at } 1380^\circ\text{C}.$$

TABLE V.

Calculated Values of the Surface Tension for Solid Nickel.

σ_L	$\sigma_{s\ M.P}$	$\sigma_{s\ 1380°C}$
1450	1630	1671
1500	1680	1721
1550	1730	1771
1600	1781	1822
1650	1831	1872
1700	1882	1923

VIII. BIBLIOGRAPHY

1. Smith, C.S., Trans. A.I.M.E., vol. 175, 1948, p. 15.

2. Harker, D. and Parker, E.R., Trans. A.S.M., vol. 34, 1945, p. 156.

3. Volmer, M. and Weber, A., Zeits. für phys. Chemie, vol. 119, 1926, p. 277.

4. Becker, R., Ann. der Physik, vol. 32, 1938, p. 128.

5. Shaler, A.J., Seminar on Kinetics of Sintering, A.I.M.E., Met. Tech., Dec. 1948.

6. Gibbs, J.W., Collected Works I, 1931, N.Y., Longmans, Green and Co.

7. Fricke, R. and Meyer, F.R., Zeits. fur phys. Chemie, vol.A 181, 1938, p. 409.

8. Hüttig, G.F., Zeits. für anorg. und allgem. Chemie, vol. 247, 1941, p. 221.

9. Chapman, J.C. and Porter, H.L., Proc. of Royal Soc., vol. A 183, 1909, p. 65.

10. Schottky, H., Gessel. Wiss. Goettingen, Nachr. Math. Phys. Klasse, vol. 4, 1912, p. 480.

11. Berggren, B., Ann. der Physik, vol. 44, 1914, p. 61.

12. Tammann, G. and Tomke, R., Zeits. für anorg. und allgem. Chemie, vol. 162, 1927, p. 1.

13. Tammann, G. and Rabe, H., Zeits. für anorg. und allgem. Chemie, vol. 162, 1927, p. 17.

14. Sawai, I. and Ueda, Y., Zeits. für anorg. und allgem. Chemie, vol. 180, 1929, p. 287.

15. Sawai, I. and Nishida, M., Zeits. für anorg. und allgem. Chemie, vol. 193, 1930, p. 133.

16. Sawai, I. and Nishida, M., Zeits. für anorg. und allgem. Chemie, vol. 204, 1932, p. 60.

17. Mack, C., Ind. Eng. Chem., vol. 27, 1935, p. 1500.

18. Sawai, I. and Nishida, M., Zeits. für anorg. und allgem. Chemie, vol. 190, 1930, p. 375.

19. Sawai, I. and Nishida, M., Zeits. für anorg. und allgem. vol. 190, 1930, p. 119.

20. Tammann, G. and Boehmem, W., Ann. der Physik, vol. 12, 1932, p. 820

21. Udin, H., Shaler, A.J., and Wulff, J., Trans. A.I.M.E., vol. 185, 1949, p. 186.

22. Udin, H., Trans. A.I.M.E., vol. 189, 1951, p. 63.

23. Funk, E.R., Udin, H. and Wulff, J., J. of Met., vol. 3, 1951, p. 1206.

24. Alexander, B.H., Kuczynski, G.C., and Dawson, M.H., Kingston, "Physics of Powder Metallurgy," p. 202, N.Y., McGraw-Hill, 1951.

25. Buttner, F.H., Udin, H., and Wulff, J., J. of Met., vol.3, 1951, p. 1209.

26. Buttner, F.H., Funk, E.R., and Udin, H., J. of Phys. and Colloid Chem.

27. Desch, C.H., J. Inst. of Met., vol. 22, 1919, p. 241.

28. Bailey, G.L.J. and Watkins, H.C., Proc. Phys. Soc., vol. B 63,1950, p. 350.

29. Buttner, F.H., Udin, H. and Wulff, J., J. of Met., vol. 5, 1953, p. 313.

30. Greenough, A.P. and King, R., J. Inst. of Met., vol. 79, 1951, p. 415.

31. Fullman, R.L., J. App. Phys., vol. 22, 1951, p. 456.

32. Hess, J.B., Unpublished work done at the Inst. for the Study of Metals, Chicago.

33. Amlinckx, S., Binnendijk, N.F., and Dekeyser, W., Physics, vol. 19, 1953, p. 1173.

34. Tolansky,S., Multiple-Beam Interferometry of Surfaces and Films, 1948, Oxford, Clarendon Press.

35. Hilliard, J.E., Unpublished work at M.I.T.

36. Harrold, J.H., and Stewart, M.B., D.R.B. Grant No. 472 and 9535-06.

37. Frenkel, J., U.S.S.R. J. of Phys., vol. 9, 1945, p. 385.

38. Kauzmann, W., Trans. A.I.M.E., vol. 143, 1941, p. 57.

39. Steigman, J., Shockely, W. and Nix, F.C., Phys. Rev., vol.56, 1939, p. 13.

40. Herring, C., J. App. Phys., vol. 21, 1950, p. 437.

41. Nabarro, F.R., Report of a Conference on the Strength of Solids, Phys. Soc. (London), 1948, p. 75.

42. Buttner, F.H., Funk, E.R. and Udin, H., J. of Met., vol. 4, 1952, p. 401.

43. Greenough, A.P., Phil. Mag., vol. 43, 1952, p. 1015.

44. Pranatis, A.L. and Pound, G.M., J. of Met., vol. 7, 1955, p. 664.

45. Stratton, R., Phil. Mag., vol. 44, 1953, p. 519 and 1236.

46. Skapski, A., Acta Met., vol. 4, 1956, p. 576.

47. Strong, J. and others, "Procedures in Experimental Physics," Prentice-Hall, 1938.

48. Forty, A.J., Adv. in Physics, vol. 3, 1954, No. 9.

49. Burgers, J.M., Proc. Kon. Ned. Ac. Wet., vol. 42, 1939, p. 293.

50. Bragg, W.L., Proc. Phys. Soc., vol. 52, 1940, p. 54.

51. Shockley, W. and Read, W.T., Phys. Rev., vol. 75, 1949, p.692.

52. Shockley, W. and Read, W.T., Phys. Rev., vol. 78, 1950, p.275.

53. van der Merve, J.H., Proc. Phys. Soc., vol. A.63, 1950, p.616.

54. Hendrickson, A.A. and Machlin, E.S., Acta Met., vol. 3, 1955, p. 64.

55. Fraser, M.J., Caplan, D. and Burr, A.A., Acta Met., vol. 4, 1956, p. 186.

56. Frank, F.C., Disc. Faraday Soc., vol. 5, 1949, p. 48.

57. Danko, J.C. and Griest, A.J., J. of Met., vol. 8, 1956, p. 515.

58. Norton, F.H. and Kingery, W.D., NYO-4631, Study of Metal-Ceramic Interactions at Elevated Temperatures.

59. Mott, N.F. and Jones, H., The Theory of the Properties of Metals and Alloys, Appendix II.